Dissociative recombination of N_2^+, O_2^+, and NO^+: Rate coefficients for ground state and vibrationally excited ions

Clint H. Sheehan[1]

Department of Physics, Ouachita Baptist University, Arkadelphia, Arkansas, USA

J.-P. St.-Maurice

Department of Physics and Astronomy, University of Western Ontario, London, Ontario, Canada

Received 10 July 2003; revised 13 January 2004; accepted 27 January 2004; published 13 March 2004.

[1] We review recent advances in the study of the dissociative recombination of molecular ions with electrons with a primary emphasis on experimental studies. In particular, we focus on previous experimental measurements of recombination rates for N_2^+, O_2^+, and NO^+ ions. In the context of this review, we present temperature dependent rate coefficients from recent merged beam studies of the dissociative recombination of N_2^+, O_2^+, and NO^+ ions with electrons. Identifying underlying physical differences between the various experimental techniques enables a discussion of the effects of vibrational excitation on the dissociative recombination of these major ionospheric species of ions. For $T < 1200$ K, we conclude that the recombination rates for N_2^+, O_2^+, and NO^+ ions in the ground electronic and vibrational states respectively are $2.2 \times 10^{-7} (T_e/300)^{-0.39}$ cm^3 s^{-1}, $1.95 \times 10^{-7}(T_e/300)^{-0.70}$ cm^3 s^{-1}, and $(3.5 \pm 0.5) \times 10^{-7}(T_e/300)^{-0.69}$ cm^3 s^{-1}. Vibrational excitation is shown to play a significant role in laboratory measurements of these recombination rates. For each of these species, vibrationally excited ions yielded a lower recombination rate than the ground state. We also discuss the recombination of these species of ions for $T > 1200$ K. *INDEX TERMS:* 2419 Ionosphere: Ion chemistry and composition (0335); 0317 Atmospheric Composition and Structure: Chemical kinetic and photochemical properties; 0335 Atmospheric Composition and Structure: Ion chemistry of the atmosphere (2419, 2427); 2407 Ionosphere: Auroral ionosphere (2704); 2459 Ionosphere: Planetary ionospheres (5435, 5729, 6026, 6027, 6028); *KEYWORDS:* recombination rates, reaction rates, ions, ionospheric composition, ionospheric chemistry, aeronomy

Citation: Sheehan, C. H., and J.-P. St.-Maurice (2004), Dissociative recombination of N_2^+, O_2^+, and NO^+: Rate coefficients for ground state and vibrationally excited ions, *J. Geophys. Res.*, *109*, A03302, doi:10.1029/2003JA010132.

1. Introduction

[2] In spite of significant advances in ionospheric modeling, some basic chemical reaction rates are still surrounded with uncertainty. In part, this is due to the apparently contradictory results presented by various earlier studies. The dissociative recombination (DR) of the main terrestrial ionospheric molecular ions, N_2^+, O_2^+, and NO^+, is a prime example of this problem. This is evidenced by the fact that the various ionospheric texts and review papers [e.g., *Banks and Kockarts*, 1973; *Schunk and Nagy*, 1980; *Rees*, 1989; *Brekke*, 1997; *Lilensten and Blelly*, 1999; *Schunk and Nagy*, 2000] present rates for these reactions which differ in both magnitude and temperature dependence. To add to the confusion, it is not uncommon in such references to have the rates presented without any identification of their source. This is a very significant problem considering that the rates found in different references may differ by as much as a factor of two. This has consequences for compositional studies of the lower ionosphere [e.g., *McNeil et al.*, 2001], as well as for attempts to understand observed electron density profiles [e.g., *Zhang et al.*, 2000]. Similarly, during electron heating events such as those observed in the auroral regions near 110 km altitude [e.g., *Schlegel and St.-Maurice*, 1981; *Wickwar et al.*, 1981], the composition can be dramatically affected through the temperature dependence of the DR rate [*Schlegel*, 1982].

[3] Clearly, it would be advantageous to uncover the causes of the differences between the published DR rates and, as a result, be able to infer which rates should be used in particular ionospheric situations. Fortunately, considerable progress has been made in recent years, both experimentally and theoretically, in our understanding of the interactions between electrons and molecular ions [e.g., *Mitchell*, 2001]. This has allowed the reconciliation of seemingly contradictory rates for a variety of species of molecular ions [e.g., *Sheehan*, 2000]. In particular, for many species of molecular ions the DR rate coefficients are now

[1]Formerly at the Merged Electron Ion Beam Experiment (MEIBE) Laboratory, Department of Physics and Astronomy, University of Western Ontario, London, Ontario, Canada.

0148-0227/04/2003JA010132

understood to be strongly dependent upon the initial state of the molecular ions.

[4] In this paper we present a review of the recent progress in the study of DR, with a focus on the DR of N_2^+, O_2^+, and NO^+. We have already addressed the DR of molecular ions of importance in Jovian ionospheres in a separate publication [*Sheehan and St.-Maurice*, 2004]. In section 2 we present an overview of the physical processes that affect the DR rate in addition to a review of recent progress made in the study of DR. In section 3 we present the results of the most recent single pass merged beam experiments with the DR of N_2^+, O_2^+, and NO^+. In view of these, and a host of earlier rates, we then discuss the causes of the differences and identify which rates should be used under various circumstances. On the basis of the discussion of section 2, we have been able to set the various rates in context and to make proposals for the best values to be used under various ionospheric conditions.

[5] A thorough review of the literature related to the DR of N_2^+, O_2^+, and NO^+ would make this paper prohibitively long. Instead, we will discuss only the most relevant references as necessary. Nevertheless, for the interested reader we have provided a catalogue of publications addressing the study of the DR of these species of molecular ions. This list of fundamental references is found in Table 1. In cases where a reference addresses multiple topics, we have listed it under each relevant heading.

2. Dissociative Recombination of Molecular Ions

2.1. Introduction

[6] In this section, we present an overview of the various interactions between electrons and molecular ions, with a particular focus on the DR process. Although in general DR is the most significant of these processes in planetary ionospheres, the ignored process of dissociative excitation may also play a significant role under certain conditions.

2.1.1. General Electron-Ion Collisions

[7] A molecular ion, AB^+, can potentially undergo any of the following reactions with an electron: radiative recombination;

$$AB^+ + e \rightarrow AB + hv, \quad (1)$$

dissociative recombination;

$$AB^+ + e \rightarrow A^* + B, \quad (2)$$

dissociative excitation (DE);

$$AB^+ + e \rightarrow A^* + B^+ + e, \quad (3)$$

or ion pair formation;

$$AB^+ + e \rightarrow A^- + B^+. \quad (4)$$

Typical radiative recombination cross sections are of the order of 10^{-20} cm^2 [*Compton and Bardsley*, 1984]. This is three to five orders of magnitude smaller than typical DR cross sections [e.g., *Mitchell*, 1990] so the process in equation (1) can be safely ignored. The process in equation (2), DR, is discussed in detail in the next subsection.

Table 1. Dissociative Recombination References

Type	Reference
	N_2^+ References
Experimental Afterglow	*Kasner* [1967]
	Mehr and Biondi [1969]
	Mahdavi et al. [1971]
	Zipf [1980a]
	Geoghegan et al. [1991]
	Canosa et al. [1991]
Experimental Shock Tube	*Cunningham and Hobson* [1972]
Experimental Merged Beam	*Mul and McGowan* [1979]
	Noren et al. [1989]
	Peterson et al. [1998]
Theoretical	*Guberman* [1989, p. 45]
	Guberman [1991]
	Guberman [1993, p. 47]
	Guberman [2003]
Branching Ratios	*Kella et al.* [1996]
	Oddone et al. [1997]
	Peterson et al. [1998]
	O_2^+ References
Experimental Afterglow	*Mehr and Biondi* [1969]
	Mahdavi et al. [1971]
	Zipf [1980b]
	Alge et al. [1983]
	Zipf [1988b]
	Spanel et al. [1993]
	Mostefaoui et al. [1999]
Experimental Ion Trap	*Walls and Dunn* [1974]
Experimental Merged Beam	*Mul and McGowan* [1979]
	Kella et al. [1997]
	Peverall et al. [2001]
Theoretical	*Guberman* [1987]
	Guberman and Giusti-Suzor [1991]
	Guberman [1997]
	Peverall et al. [2000]
Branching Ratios	*Abreu et al.* [1983]
	Killeen and Hays [1983]
	Guberman [1987]
	Queffelec et al. [1989]
	Yee et al. [1989]
	Takahashi et al. [1990]
	Guberman and Giusti-Suzor [1991]
	Sobral et al. [1992]
	Guberman [1997]
	Kella et al. [1997]
	Peverall et al. [2000]
	Peverall et al. [2001]
	NO^+ References
Experimental Afterglow	*Gunton and Shaw* [1965]
	Young and St. John [1966]
	Weller and Biondi [1968]
	Mahdavi et al. [1971]
	Huang et al. [1975]
	Alge et al. [1983]
	Spanel et al. [1993]
	Mostefaoui et al. [1999]
Experimental Shock Tubes	*Davidson and Hobson* [1987]
Experimental Ion Trap	*Walls and Dunn* [1974]
Experimental Merged Beams	*Mul and McGowan* [1979]
	Vejby-Christensen et al. [1998]
Theoretical	*Bardsley* [1968]
	Michels [1975]
	Lee [1977]
	Bardsley [1983]
	Sun and Nakamura [1990]
	Rabadan and Tennyson [1996]
	Rabadan and Tennyson [1997]
	Rabadan and Tennyson [1998]
	Valcu et al. [1998]
	Schneider et al. [2000]
Branching Ratios	*Kley et al.* [1977]
	Vejby-Christensen et al. [1998]

[8] The process in equation (3), DE, must be treated with caution and cannot always be neglected. For example, recent storage ring experiments have shown that for NO^+, DE begins to dominate over DR at electron energies greater than 12 eV [*Vejby-Christensen et al.*, 1998]. Beyond 15 eV, the DE cross section exceeds the DR cross section by at least one order of magnitude. Similar results were also observed for O_2^+ [*Peveral et al.*, 2001] and N_2^+ [*Peterson et al.*, 1998]. Experiments such as these demonstrate that for diatomic molecular ions at least, the DE cross section as a function of collision energy loosely resembles a step function. The cross section jumps steeply from negligible values to near maximal values in the neighborhood of 10 eV. Once these maximal values have been reached, the DE cross section remains nearly constant as the collision energy increases.

[9] DE may therefore be a significant process in planetary ionospheres, for instance, during auroral conditions when electrons impact molecular ions with energies in excess of 10 eV. Being a source of atomic ions and excited atoms, the DE process could alter the ionospheric composition, and may even be an important factor in auroral emissions. It should also be noted that DE is not a sink of electrons, since the incident electron remains unbound after the interaction. It is curious, in this respect, that DE is a process that is seemingly completely ignored in ionospheric studies, at least as evidenced by the standard texts and reviews such as those cited above in the introduction. We are planning future studies to investigate the impact of DE upon the composition and dynamics of the auroral ionosphere.

[10] The process in equation (4), ion pair formation, proceeds in a similar way to DR [*Le Padellec et al.*, 2001]. An electron is captured by a molecular ion forming an excited neutral molecule that subsequently dissociates. The difference is that with this process the dissociation products are electrically charged, whereas the DR products are neutral. The process of ion pair formation has been sparsely studied to date. Of relevance to ionospheric research is a recent study of ion pair formation in the recombination of NO^+ with electrons [*Le Padellec et al.*, 2001]. They observed the total ion pair formation cross section to be negligible for collision energies below approximately 10 eV and above approximately 18 eV. Within the 10–18 eV range, cross sections ranged from 10^{-19} cm^2 to 10^{-18} cm^2, with a sharp peak at 12.5 eV. These are similar to the results observed in experiments with HD^+ and HF^+ [*Zong et al.*, 1999], and with HD^+ and OH^+ [*Larson et al.*, 2000].

[11] A comparison of the storage ring cross sections from the DR of NO^+ [*Vejby-Christensen et al.*, 1998] with those of ion pair formation from NO^+ [*Le Padellec et al.*, 2001], for the 10–18 eV range, reveals that the DR cross sections are consistently greater than the ion pair formation cross section by approximately two orders of magnitude. Thus as far as NO^+ chemistry is concerned, ion pair formation in the ionosphere can be neglected. Since the cross sections for the other diatomics listed above are similar to those of NO^+, it seems reasonable to assume that ion pair formation can also be neglected for O_2^+ and N_2^+ chemistry. Nevertheless, there is a need for experimental studies of ion pair formation for the latter two species.

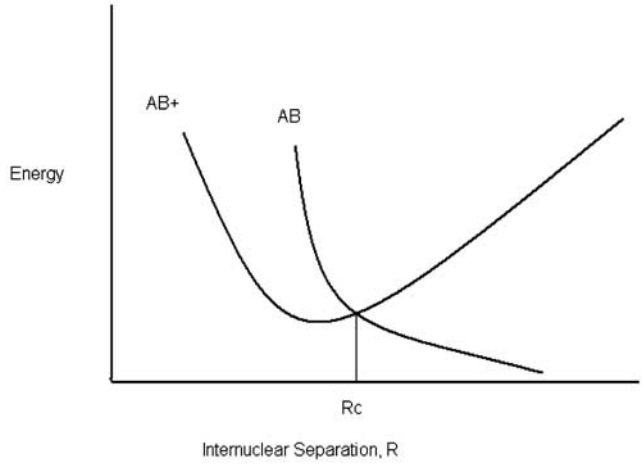

Figure 1. Direct process dissociative recombination illustrated using potential curves for a simple two-state system consisting of a bound ionic state AB^+ and a neutral dissociating state AB.

2.1.2. An Overview of the Dissociative Recombination Process

[12] While equation (2) is the typical way of expressing the DR process, it is in fact an oversimplification. The process is more accurately represented by

$$AB^+ + e \leftrightarrow AB^{**} \rightarrow A^* + B. \quad (5)$$

The capture of an electron by an ion AB^+, leading to the formation of the excited neutral molecule AB^{**} as indicated in equation (5), can take place in a single step (direct process) or in two steps (indirect process). A detailed discussion of the differences between the direct and indirect processes is beyond the scope of this paper. There are a number of good discussions of this topic [e.g., *McDaniel et al.*, 1993, pp. 567ff.]. We will therefore only review the basics of each process.

[13] DR is an electronic correlation problem [*Linderberg*, 1998] and the general idea can be understood by examining the diagram in Figure 1. This diagram shows a simplistic two-state system consisting of a bound ionic state, AB^+, and a high lying neutral repulsive state, AB. Since the potential curve of AB has no local minimum, it represents an unbound state. A molecule in this state AB will dissociate to A + B as the internuclear separation increases. Above the state AB^+ lies the continuum AB^+ + e. When an electron collides with an ion in AB^+, it can be captured into the neutral state AB provided that the sum of the energy of the ion at that internuclear separation and the energy of the incident electron is equal to the energy of the neutral state at the same internuclear separation. Since the neutral capture state lies above the ion state, it is unstable. This system can either be stabilized through autoionization or DR. The neutral curve crosses the ion curve at a critical internuclear separation, labeled R_c. For $R < R_c$, the state AB lies above the ionization threshold and is therefore autoionizing, meaning it may spontaneously re-emit the captured electron. For $R > R_c$, however, the state AB is a lower-energy state than the ionic state and autoionization is no longer energet-

ically possible. In this case, the recombination proceeds through the dissociation of the molecule.

[14] Qualitatively, the DR cross section for the direct process is given by [*Mitchell*, 1990]

$$\sigma = \left(\frac{\Gamma}{E}\right)(FC)(S), \tag{6}$$

where Γ is the resonance capture width which describes the strength of the capture process, E is the incident electron kinetic energy, FC is the Franck-Condon factor which describes the overlap of the nuclear wave functions of the initial ion state and the repulsive neutral state, giving the probability of transition from the initial to the final state, and S is the survival factor which indicates the probability of the recombination being stabilized by dissociation rather than decaying by autoionization. For cases of good overlap (FC = 1) and efficient stabilization (S = 1), the energy dependent cross sections are proportional to E^{-1}. If, however, the overlap is poor, then the Franck-Condon factor will be energy-dependent and the cross sections will no longer simply be proportional to E^{-1}. This is because the FC term in equation (6) would become the second energy-dependent term in the cross section, in addition to the E in the denominator. For stability reasons, the most probable internuclear separation for an ion in state AB^+ is at the minimum of the potential curve. Therefore the overlap integral, and in turn the Franck-Condon factor, are maximized when the neutral repulsive curve crosses the ionic curve near its minimum. Thus the closer the curve crossing is to optimal, the higher the DR cross section will be.

[15] This discussion of the direct process is easily extended to account for the initial vibrational state of the ions. Again, we will consider a simplistic case. In Figure 2, v is some vibrational level of the ionic state AB^+, while AB_1 and AB_2 are two repulsive neutral states. A molecule in a vibrational state v spends most of its time near the classical turning points. These therefore represent the most probable

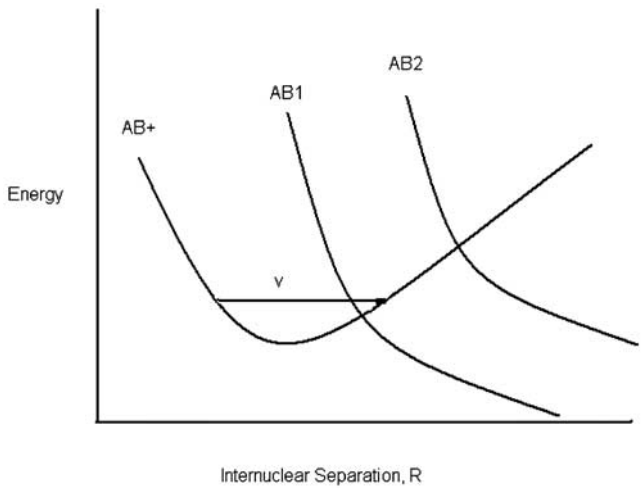

Figure 2. Dissociative recombination of vibrationally excited ions illustrated using potential curves for a simple system consisting of a vibrational level v of a bound ionic state AB^+ and two neutral dissociating states AB_1 and AB_2.

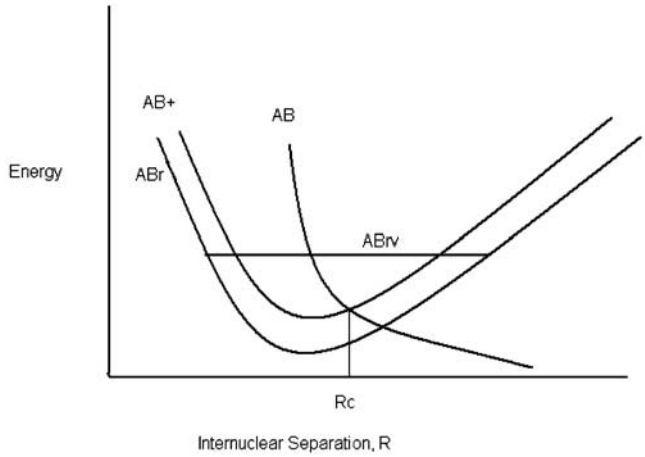

Figure 3. Indirect process dissociative recombination illustrated using potential curves for a simple system consisting of a bound ionic state AB^+, a Rydberg state AB_R, a vibrational level of the Rydberg state AB_{Rv}, and a neutral dissociating state AB.

internuclear separations of the ion AB^+. From this it follows that the Franck-Condon factor will be maximized when a neutral repulsive curve crosses the vibrational level of the ion between the turning points. Thus in Figure 2, AB_1 exhibits a more optimal curve crossing than AB_2. Since each molecular species will have a unique set of neutral and ionic curves, it is evident that no general rule can be stated for the dependence of the DR cross section upon the vibrational excitation of the ion. Each species must be dealt with on an individual basis. For instance, it has been observed that the DR cross section decreases with increasing vibrational excitation for NO^+ [e.g., *Mostefaoui et al.*, 1999], while for H_2^+ the cross section increases with increasing vibrational excitation [e.g., *Hus et al.*, 1988a]. Thus vibrational excitation can either enhance or suppress the DR process, depending on the species of ions.

[16] The indirect process is somewhat more complicated. Figure 3 illustrates the indirect process. Each electronic state of a molecular ion represents the limit of a Rydberg series of neutral states. A Rydberg state of a molecule AB (labeled AB_R in Figure 3) lying close to the limiting ion state AB^+ can have vibrationally excited levels (labeled AB_{Rv} in Figure 3) above the state AB^+. An ion in the state AB^+ can therefore capture an electron of suitable energy into the vibrationally excited rydberg state AB_{Rv}. Since this capture state lies above the ionization limit, autoionization is one possible outcome. If a neutral repulsive state AB crosses this capture state as indicated in Figure 3, a second possible outcome is that the molecule will dissociate due to the capture state being predissociated by AB. The indirect process is represented by

$$AB^+ + e \Leftrightarrow AB_{Rv} \rightarrow AB \rightarrow A + B. \tag{7}$$

[17] Interestingly, for the first time, the differences between the direct and indirect processes (HCN^+/HNC^+ isomers) have now been observed experimentally [*Sheehan et al.*, 1999; *Talbi et al.*, 2000]. The direct process has been found to be the considerably more efficient of the two, with

a rate coefficient nearly 30 times larger than that for the indirect process in this instance.

2.2. Review of Recent Progress

[18] In the pioneering days of the study of DR, experimental techniques such as stationary afterglows, shock tubes, flames, and ion traps were used. These techniques, along with their strengths and weaknesses, have been reviewed in detail elsewhere [*McDaniel et al.*, 1993, pp. 573–583]. The primary weaknesses of these early methods involved the inability to account for initial ionic states, as well as the problem of reaction rates being influenced by the presence of chemical impurities and competing processes. The majority of these problems associated with the earlier techniques have been solved following the advent of the flowing afterglow Langmuir probe (FALP) technique and the merged beams technique.

[19] With the FALP approach [e.g., *Mostefaoui et al.*, 1999], molecules are chemiionized and then drawn along a drift tube by a roots pump. The ions and their accompanying electrons flow together down the drift tube in a stream of neutral buffer gas. A movable Langmuir probe measures the electron density along the axis of the drift tube. From the decay in the electron density, the DR rate coefficient is determined. An obvious potential problem is the presence of impurity ions that can significantly alter the observed reaction rates. This problem has been accounted for in the FALP apparatus at the University of Rennes in France by the addition of a movable quadrupole mass spectrometer [*McDaniel et al.*, 1993, p. 575]. By moving the mass spectrometer along the flow with the Langmuir probe, the researchers have been able to identify and measure the number density of impurity ions. This provides a significant improvement over earlier techniques. Another significant advantage of the FALP technique over most others is the ability to study vibrationally relaxed ions due to collisional quenching arising from the elevated pressures in the apparatus [*Mitchell*, 1990]. A particular advantage of the FALP technique over the stationary microwave afterglow technique [e.g., *Mehr and Biondi*, 1969] is that in the FALP apparatus the ion formation region and the electron-ion interaction region are separated. This minimizes such stationary afterglow technique problems as spatial inhomogeneities in the electron energy distribution, non-Maxwellian distributions, and the vibrational excitation of the reactant ions [*Mitchell*, 1990].

[20] The higher gas pressures in a FALP experiment provide an advantage over techniques performed in high vacuum regions owing to the facilitation of vibrational relaxation of the ions. These higher pressures can also introduce potential complications. The resulting lower mean collision time may enhance other reactions. For example, it is conceivable that the three body process

$$AB^+ + e + X \rightarrow AB + X \qquad (8)$$

could become significant. The resulting higher electron density decay rates would in turn produce an observed DR rate coefficient that is too large.

[21] The introduction of the merged beams approach to studying DR in the late 1970s has shed considerable light on the subject. With this approach, parallel ion and electron beams are first tuned to produce very small relative velocities and are then electromagnetically merged. There are several advantages to the merged beams approach compared with other techniques. First, this technique ensures that the interactions involve only one well-defined ion with respect to mass [*Mitchell and Rebrion-Rowe*, 1997]. Second, this method enables the observation of reaction cross sections as a function of collision energy for energies ranging from a few meV to tens of eV with very high resolution [*Mitchell*, 1990; *Sheehan*, 1996]. This high resolution of collision energy arises from transforming the velocities of the beam particles from the laboratory frame to the center-of-mass frame. This transformation of reference frames effectively deamplifies the energy spread of the beams. This allows many details to be observed that are lost or obscured by the other methods in which the rate coefficient, rather than cross sections, is the measured quantity. For example, the merged beams approach has been used successfully to demonstrate complex cross-section structure most likely due to interfering Rydberg states [e.g., *Hus et al.*, 1988b; *Van der Donk et al.*, 1991; *Schneider et al.*, 1997], the opening of additional product channels [e.g., *Le Padellec et al.*, 1997], and the identification of different specific vibrational states [e.g., *Hus et al.*, 1988a]. In conjunction with new imaging and detection technology, this technique has also been successfully used to determine the branching ratios for the different product channels [e.g., *Amitay et al.*, 1996; *Kella et al.*, 1996; *Larson et al.*, 1998]. The main weakness of the merged beams approach is that the ions are typically produced in electron impact ionization sources resulting in the population of many vibrational states [e.g., *Zajfman and Amitay*, 1995]. We will discuss the implications of this in section 3.

[22] Merged beams experiments have been described in considerable detail in a number of references [e.g., *Phaneuf et al.*, 1999]. There are two variations of merged beams experiments, single pass and multipass. In a single pass experiment, the ions and electrons are merged once, while in a multipass experiment, the ions are merged with electrons millions of times per second. The first successful merged beams studies of DR were performed in the late 1970s in the Merged Electron Ion Beam Experiment (MEIBE) lab in the Department of Physics and Astronomy at the University of Western Ontario. We obtained the single pass results reported later in this paper in the MEIBE lab. For this reason, we provide a more detailed discussion of the MEIBE apparatus in the following section.

[23] Motivated by the success of earlier single pass merged beams experiments, multipass DR experiments were first performed in the early 1990s. This refinement to the merged beams approach was enabled by the development of heavy ion storage rings. The multipass technique has been described in detail in a number of articles [e.g., *Le Padellec et al.*, 1999]. Briefly, ions are injected into a large storage ring and accelerated. The ion beam circulates at MHz frequencies with a typical ion energy of a few MeV. The ion-electron interactions occur each revolution in a straight section of the storage ring. The unreacted ions continue to circulate while the neutral products travel undeflected to the appropriate detection system.

[24] The multipass approach enjoys several advantages over the single pass approach. First, since the ions and

electrons collide millions of times each second, the ion-electron collision rate is much higher in a multipass system. Thus considerably less observing time is required to obtain suitable counting statistics with a multipass system.

[25] The second significant advantage of the multipass approach over the single pass approach is the improved ability to produce beams of ground state ions. Relaxation times for the radiative vibrational relaxation of heteronuclear diatomic molecular ions typically fall in the range of milliseconds to a few seconds [*Amitay et al.*, 1994]. Since the ion beam circulates in a storage ring for times of the order of a few seconds, the ions normally have time to relax into their ground electronic and vibrational states. In contrast, the time from creation to interaction for ions in the MEIBE single pass apparatus is of the order of 10^{-4} s. This results in a higher probability of the population of vibrationally excited states within the single pass ion beam. The important exception is ion species that lack an electric dipole moment, such as the homonuclear diatomics. Lacking a dipole moment, such ions are infrared inactive and therefore have vibrational lifetimes that can be hours or longer [*Zajfman and Amitay*, 1995]. For example, the lifetime estimated for the transition to the ground vibrational state of H_2^+ from the first excited vibrational level is on the order of 10^6 s [*Peek et al.*, 1979].

[26] In spite of the advances presented by the multipass approach, the single pass approach is not without its advantages. In the MEIBE lab we directly measured cross sections as a function of collision energy. These cross sections can then be integrated over any distribution function of interest to obtain the relevant rate coefficients. The multipass groups, however, directly measure the reaction rate as a function of collision energy. The cross section as a function of energy is then mathematically extracted from the energy dependent rates. Finally, the temperature dependent rate coefficients are determined from the extracted cross sections [e.g., *Amitay et al.*, 1996]. This extra step can introduce additional uncertainties into the calculations.

[27] The single pass MEIBE apparatus always enables a precise determination of absolute beam currents and energies. This in turn allows the determination of absolute cross sections. With the multipass experiments, however, there at times is difficulty in determining ion counts and currents [e.g., *Amitay et al.*, 1996; *Vejby-Christensen et al.*, 1997]. As a consequence, multipass experiments are sometimes only able to yield relative cross sections. In such cases, the calculation of temperature dependent rate coefficients would be meaningless.

[28] Although the multipass approach makes the study of ground state ions easier due to prolonged beam storage times, this can make the study of excited ions with a multipass experiment more difficult. Conversely, the short time from production to interaction in single pass experiments makes the study of ions in excited states easier. This makes obvious the advantage of collaborations between multipass and single pass groups to obtain a fuller understanding of the physics and chemistry of molecular ions. Recognizing the physical differences between the single pass and multipass merged beam methods, researchers from both groups have cooperated closely to develop a deeper understanding of the DR process for various species of molecular ions [e.g., *Le Padellec et al.*, 1998; *Le Padellec et al.*, 1999].

2.3. MEIBE Single Pass Merged Beam Experiment

[29] The MEIBE apparatus and procedures have been described elsewhere in full detail [*Auerbach et al.*, 1977; *Keyser et al.*, 1979] so we only present a brief overview. The ions are produced by the impact of 100 eV electrons upon neutral molecules inside a standard rf ion source mounted at the high voltage terminal of a van der Graaff accelerator. The van der Graaff accelerates these ions to energies of 350 keV. The species of interest is mass selected using a bending magnet and the ion beam is injected into the beam line. Before arrival at the interaction region, the ion beam is electrostatically deflected twice to eliminate any fast neutrals produced in flight through charge exchange reactions between the beam ions and the background gas during injection.

[30] The electrons are produced by a planar diode type electron gun. Specifically, a ceramic-coated tungsten filament indirectly heats a barium oxide cathode causing it to emit electrons. The filament is shielded by the cathode so that no electrons emitted from the filament are able to contaminate the electron beam. The electrons are accelerated to the desired energy that typically falls into the range of 10–100 eV, depending on the mass of the ion species. Next, the electron beam is electrostatically focused to overcome space charge effects. The trajectory of the electron beam through the vacuum chamber is initially parallel to that of the ion beam. The electron beam is then laterally displaced using crossed electric and magnetic fields. By adjusting these fields, the beams are merged for a distance of 86 mm within the interaction region. The ions are too massive to be measurably displaced by these fields and so they effectively retain their original trajectory. After exiting the interaction region, the electron beam is separated out by a second set of crossed electric and magnetic fields. The electrons continue on their new trajectory to a Faraday cup for collection. The neutral beam particles continue in a straight line to a silicon surface barrier detector where they are detected and counted. A single channel analyzer is used to set a window at full beam energy for the neutral detector, corresponding to the neutral products of DR. The ions are electrostatically deflected away from the neutrals and collected by a second Faraday cup.

[31] Even though this experiment is performed inside an ultra-high vacuum region in which a pressure of 10^{-9} Torr is maintained, charge exchange reactions between the beam ions and the residual background particles still produce a significant number of fast neutrals. Since these fast neutrals have the full beam energy, they register as a DR signal at the neutral detector. To account for this, the electron beam is modulated so that effectively it is on for 50% of the time and off for 50% of the time. Two digital scalers are used to obtain neutral counts both in and out of phase with this modulation. The scaler in phase with the electron beam provides the signal plus background count (S + B), while the scaler out of phase provides only the background count (B). Taking the difference between these two counts yields the true signal. We obtain the collision cross-section from experimental parameters according to

$$\sigma = \frac{C_n e^2}{I_i I_e L} \left| \frac{v_i v_e}{v_e - v_i} \right| F, \tag{9}$$

where C_n is the neutral count rate, I_i and I_e are the ion and electron beam currents, L is the length of the interaction region, v_i and v_e are the ion and electron lab frame velocities, and F is the form factor [*Auerbach et al.*, 1977].

[32] Ideally, the ion and electron beams would overlap perfectly through the interaction region. In reality however, this is not the case. The form factor, *F*, in equation (9) corrects the cross section for this by accounting for the true beam overlap. The form factor is given by

$$F = \frac{\iint j_e(x,y)dxdy \cdot \iint j_i(x,y)dxdy}{\iint j_i(x,y)j_e(x,y)dxdy}, \tag{10}$$

where j_e and j_i are the electron and ion beam current densities. Experimentally, the form factor is determined by scanning the beams at three different locations over the length of the interaction region with a set of knife-edge scanners (see *Keyser et al.* [1979] for full details).

[33] The largest source of uncertainty in the calculation of the cross section from equation (9) is the neutral count rate. As stated above, the true neutral signal will be given by

$$S_{true} = (S + B) - (B). \tag{11}$$

This represents the total number of neutral counts for a given run and it is equivalent to integrating the neutral count rate C_n over the entire counting time of the run. As a counting experiment, this follows Poisson statistics and so the uncertainty in the true neutral signal is

$$\delta S_{true} = \sqrt{S + 2B}. \tag{12}$$

For the new MEIBE data presented in this paper, the average uncertainty in the neutral count was 10%. A recent systematic analysis of the operation and calibration of all components of the MEIBE apparatus has determined that the remainder of the parameters in equation (9) contributes a maximum of 6% to the uncertainty in the experimentally determined cross section [*Sheehan*, 2000].

[34] From the energy-dependent cross sections, a temperature dependent rate coefficient for any relative speed distribution of interest, f(v), is obtained by evaluating

$$\alpha(T_e) = \int_0^\infty v\sigma(v)f(v)dv. \tag{13}$$

We calculated all of our rates by evaluating equation (13) using the Maxwellian distribution

$$f(v) = \frac{4}{\pi^{1/2}}\gamma^{3/2}v^2\exp(\gamma v^2), \tag{14}$$

where

$$\gamma^{-1} = \frac{2k_BT_e}{m_e}. \tag{15}$$

In the future, we plan to revisit this problem for cases where there are departures from Maxwellian distributions. A statistical analysis of the variance of the calculated rate coefficient based on an uncertainty of 20% in our experimentally determined cross-sections sets the uncertainty in the rate coefficients we report in section 3 at ±15%.

[35] By the middle of the 1990s, as more multipass DR data became available, an apparent discrepancy arose between the single pass and multipass merged beams experiments. In some instances, for example CH_3^+ and H_3O^+ [*Vejby-Christensen et al.*, 1997], the new multipass results were nearly identical to the older single pass results. However for some other species, such as CN^+ [*Le Padellec et al.*, 1999], the new multipass results differed significantly from the earlier single pass results. The question was why two fundamentally identical experiments were yielding differing results. There was obviously not a systematic flaw in either approach since the agreement was excellent for some species of ions. There could not have been a systematic error in either calibration or calculation since where differences in data did exist, the differences were not consistent from one species to another. This issue led to a comprehensive multiyear review of the MEIBE lab [*Sheehan*, 2000]. This review included the confirmation of the proper functioning of all components of the apparatus. The proper calibration of each component of the detection and counting systems was also confirmed, including a novel measurement of the efficiency of a silicon surface barrier detector [*Sheehan et al.*, 2000]. In conclusion we determined that the maximum uncertainty in the electron current measurement was 1%, and the maximum uncertainty in the ion count was 5%. Counting statistics typically added an additional 5–15% uncertainty to the cross sections through the neutral count, as discussed above.

[36] After we had confirmed that the MEIBE apparatus was properly functioning and calibrated, and once the bounds of accuracy were determined, several earlier MEIBE experiments were repeated. In all cases, the new results were consistent with the previously published MEIBE results. This indicated that there must be some underlying physical explanation for the differences that existed in certain cases between MEIBE results and storage ring results. In the next section of this paper, we present these new MEIBE results for N_2^+, O_2^+, and NO^+ along with a discussion of the reason they differ from storage ring results. The discussion will be extended to include FALP results and theoretical calculations where possible. We will demonstrate that the apparently contradictory rates reported by various studies can be understood on the basis of ions in differing initial states.

3. N_2^+, O_2^+, and NO^+ DR Rate Coefficients

3.1. Introduction

[37] The differing DR rate coefficients for each of N_2^+, O_2^+, and NO^+ provide a window into a deeper understanding of the DR process for these species of molecular ions. A recent study of the effects of the internal energy of the ions on the DR process [*Sheehan*, 2000] has shown that the differences between the various published experimental rate coefficients can be explained in terms of differences in internal ion energies arising from the use of different experimental techniques. As we discuss in more detail below, multiple rates obtained with a given technique tend to be consistent. The differences in reported rates tend to be from one experimental technique to another.

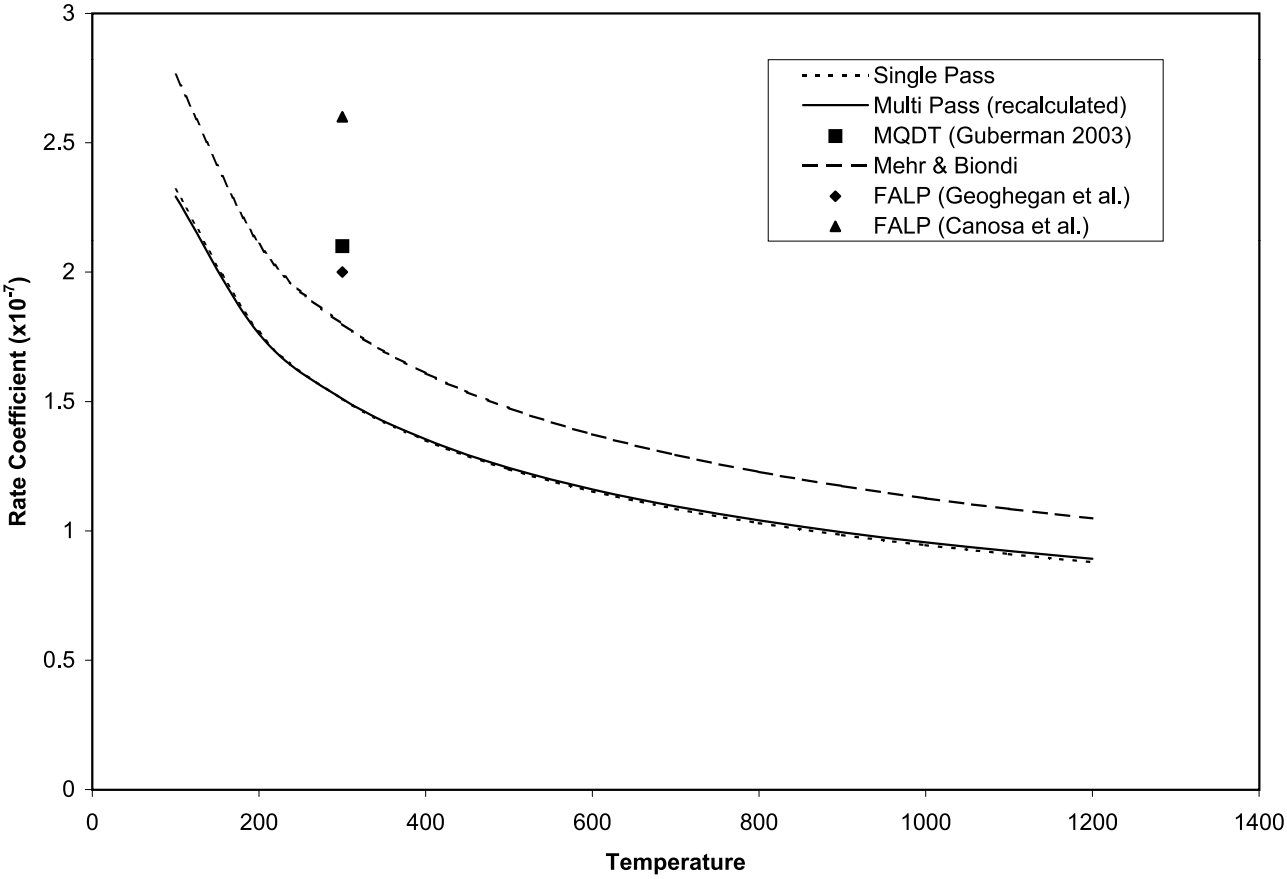

Figure 4. Rate coefficients for the dissociative recombination of N_2^+ for $T_e < 1200$ K.

[38] The new single pass results we report here are in good agreement with the original MEIBE work of *Mul and McGowan* [1979]. By analyzing the various rate coefficients in light of the specific experimental techniques through which they were obtained, we can arrive at a fuller understanding of the DR process for specific species of ions. This allows researchers a higher level of confidence in their selection of the rates most appropriate for their specific studies.

3.2. Dissociative Recombination of N_2^+

[39] The rate coefficients of interest for the DR of N_2^+ for $T_e < 1200$ K are in Figure 4 and Table 2. The analysis of these is followed by a discussion of rates for higher temperatures. To make comparisons more meaningful, we have tried to provide uncertainties for all of the rates discussed in this paper. Some were stated explicitly in the original sources; we estimated others based on information found within the original sources.

[40] If all other collision processes in an electron impact ionization source are neglected, then the vibrational levels of the resulting ions will be populated according to the Franck-Condon distribution [*Schmidt et al.*, 1996]. This distribution for the formation of N_2^+ from N_2 by the impact of 100 eV electrons has been calculated elsewhere [*Noren et al.*, 1989] and the results are presented in Table 3. We conclude from the short residence time of our ions in the MEIBE ion source that this distribution should be a reasonable reflection of the population profile of our N_2^+ beam. With this ion beam, we observed a temperature dependent rate coefficient of $1.5 \times 10^{-7}(T_e/300)^{-0.39}$ cm^3 s^{-1}.

[41] The multipass results quoted in Table 2 were obtained at the CRYRING facility in Stockholm [*Peterson et al.*, 1998]. Since N_2^+ does not have a dipole moment, beam storage times are not sufficient to achieve significant vibrational cooling. Therefore in an attempt to produce cool

Table 2. N_2^+ DR Rate Coefficients ($T_e < 1200$ K)

Source	Rate Coefficient, cm^{3}s^{-1}
Single Pass	$(1.50 \pm 0.23) \times 10^{-7}(T_e/300)^{-0.39}$
Multipass (Recalculated)	$(1.5 \pm 0.23) \times 10^{-7}(T_e/300)^{-0.38}$
MQDT	2.1×10^{-7} at T = 300 K
Mehr and Biondi	$(1.8 \pm 0.4) \times 10^{-7}(T_e/300)^{-0.39}$
FALP (Geoghagen et al.)	2.0×10^{-7} at T = 300 K
Zipf	2.2×10^{-7} at T = 300 K
FALP (Canosa et al.)	2.6×10^{-7} at T = 300 K

Table 3. Population of Vibrational States of N_2^+ From Impact of 100 eV Electrons on N_2

Vibrational State	Population
0	0.651
1	0.211
2	0.084
3	0.035
4	0.013
5	0.005
6	0.001

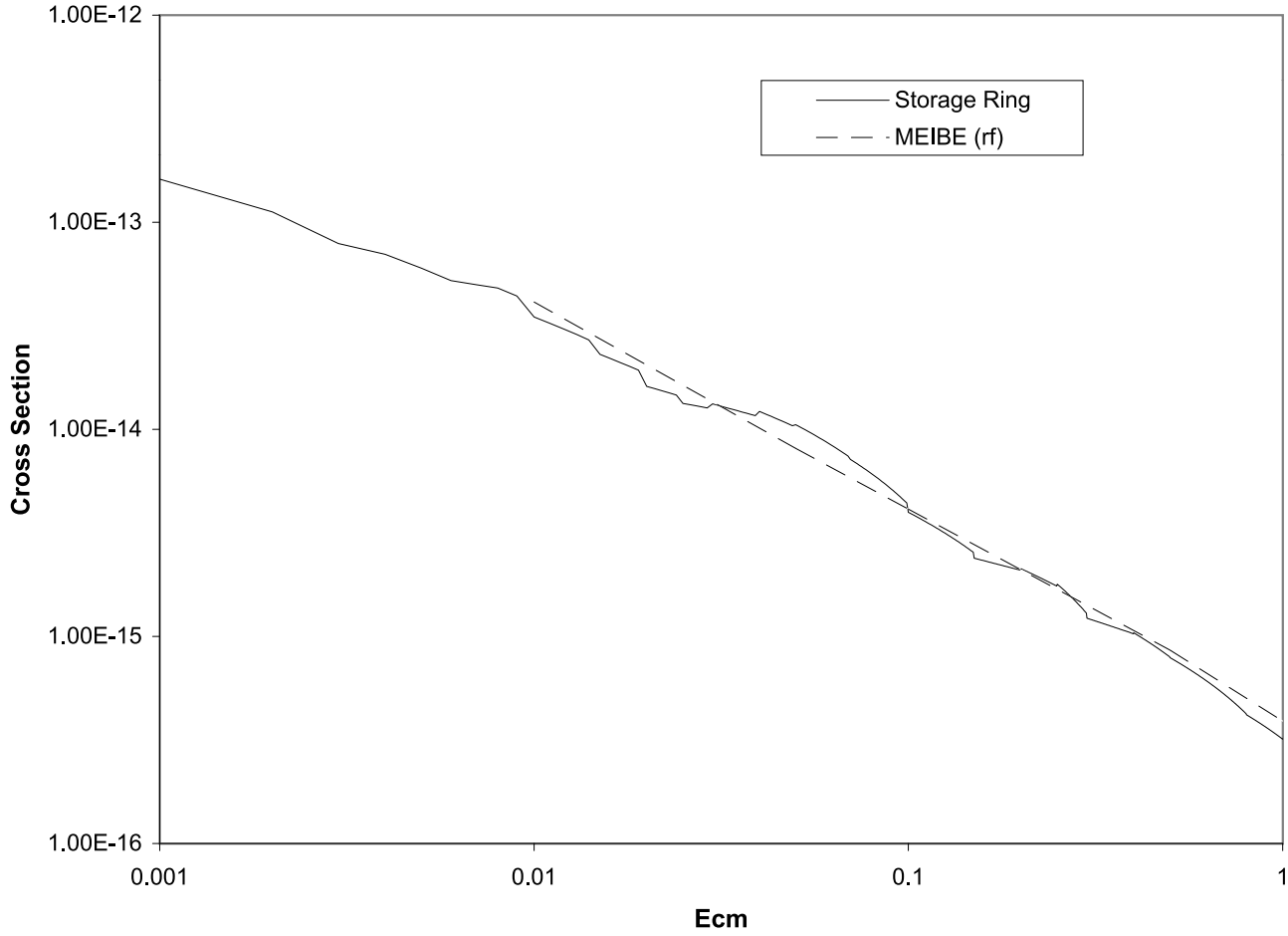

Figure 5. Energy dependent cross-sections for the dissociative recombination of N_2^+ for single pass and multipass experiments compared.

ions, a special high-pressure hollow cathode source was utilized to enhance collisional quenching, since

$$N_2^+(v^*) + N_2(v=0) \Leftrightarrow N_2(v^*) + N_2^+(v=0) \qquad (16)$$

is known to be a highly efficient process [*Lindinger et al.*, 1981; *Smith and Adams*, 1981]. This resulted in an ion beam with an observed population of 46% v = 0, 27% v = 1, 10% v = 2, and 16% v = 3. Comparing this population with the one of Table 3 indicates that the multipass and single pass N_2^+ beams had similar vibrational populations. This accounts for the similar observed rate coefficients.

[42] The divergence between the *Peterson et al.* [1998] rate coefficient of $1.75 \times 10^{-7}(T_e/300)^{-0.30}$ cm^3 s^{-1} and our MEIBE rate presented above was somewhat surprising since the two sets of cross sections were nearly identical (see Figure 5). After recalculating our rate coefficient, we decided to calculate the rate coefficient from their cross sections. In doing so, we obtained a value of $1.5 \times 10^{-7}(T_e/300)^{-0.38}$ cm^3 s^{-1}. Given the above discussion of the similarities in ion beam populations with these two experiments, the similarities in the cross sections and the theoretical temperature dependence of the rate [*Guberman*, 1991; *Guberman*, 1993], this recalculated value is not a surprise.

[43] *Mehr and Biondi* [1969] obtained their results using a microwave afterglow apparatus. The high number densities and pressures in afterglow experiments result in the very efficient collisional quenching of the vibrationally excited states of N_2^+ by N_2 [*Geoghegan et al.*, 1991]. The N_2^+ ions in the experiments of Mehr and Biondi should therefore almost exclusively have been in the ground vibrational state. They noted that their results must, however, be interpreted with caution. They reported a problem with contamination by N_3^+ and N_4^+ ions, which they were unable to eliminate. Their analysis suggested that given the lower recombination rate for these heavier ions, the observed N_2^+ rate coefficient of $1.8 \times 10^{-7}(T_e/300)^{-0.39}$ cm^3 s^{-1} might need to be adjusted upwards by up to 10%. This correction is reflected in their paper by the use of a larger upper error bar.

[44] The difficulties encountered by *Mehr and Biondi* [1969] are fully resolved using a FALP apparatus. The moveable Langmuir probe allows measurements of electron densities along the flow tube and a quadrupole mass spectrometer is used to precisely determine the ion species present in the plasma. Two groups to date have used the FALP technique to study the DR of N_2^+ in the vibrational ground state. These groups reported rate coefficients at 300 K of 2.0×10^{-7} cm^3 s^{-1} [*Geoghegan et al.*, 1991] and 2.6×10^{-7} cm^3 s^{-1} [*Canosa et al.*, 1991], respectively.

[45] The value quoted by *Schunk and Nagy* [2000], without reference, appears to be the v = 0 value reported

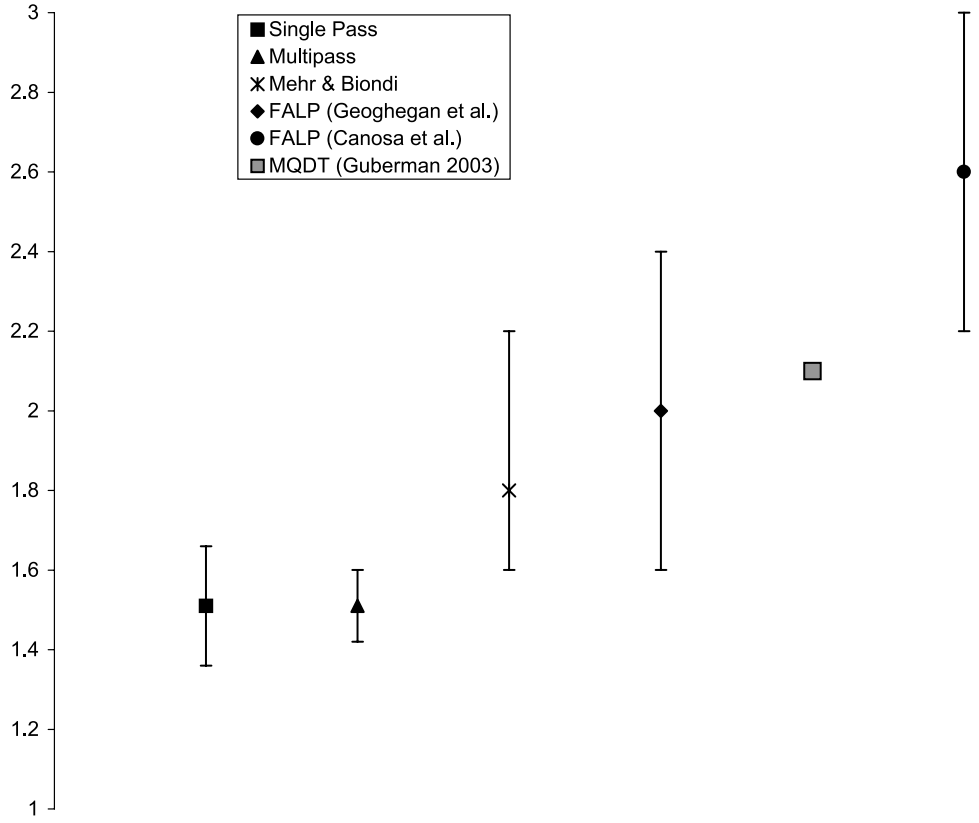

Figure 6. Experimental rate coefficients for the dissociative recombination of N_2^+ at T_e = 300 K.

by *Zipf* [1980a, 1980b], who used a microwave afterglow coupled with a laser induced fluorescence setup. Zipf presented rate coefficients as a function of vibrational state for v = 0 up to v = 2, reporting 2.15×10^{-7} cm^3 s^{-1} for v = 0, 2.42×10^{-7} cm^3 s^{-1} for v = 1, and 2.70×10^{-7} cm^3 s^{-1} for v = 2, all at 300 K. The original interpretation of these results as representing vibrationally resolved rates has now been challenged by a growing number of researchers. The original data analysis had not accounted for the strong resonant charge exchange process of equation (16). Since the N_2 and N_2^+ both probably had a vibrational temperature of 1500 K, Zipf's measurements likely reflected the effective recombination rate for an N_2^+ gas with a vibrational temperature of 1500 K, rather than vibrationally resolved rates [*Johnsen*, 1987]. A reanalysis of Zipf's data, accounting for resonant charge exchange based on Johnsen's discussion, resulted in a v = 0 rate at 300 K of approximately 2.6×10^{-7} cm^3 s^{-1} [*Bates and Mitchell*, 1991]. This reanalysis also demonstrated that the recombination rate decreases as v increases from 0 to 2.

[46] In light of this brief discussion of the various rates, Figure 4 provides a wealth of information about the DR of N_2^+. One obvious feature of this plot is the fact that all of the rates, experimental and theoretical, have a nearly identical temperature dependence of $T_e^{-0.39}$. This implies that for N_2^+ the temperature dependence of the DR rate coefficient is independent of vibrational excitation for T_e < 1200 K.

[47] While the temperature dependence of the N_2^+ DR rate coefficient is not observed to vary with vibrational excitation, the magnitude of the rate is seen to depend on the excitation of the ions. Figure 6 presents the experimental rate coefficients, with uncertainties, at 300 K. There is little doubt that both FALP rates reflect ground state ions. Similarly, *Mehr and Biondi* [1969] make a convincing case that their results were obtained with ground state N_2^+ ions. The longer upper error bar on their value in Figure 6 reflects their attempt to account for the observed presence of N_3^+ and N_4^+ impurities as discussed above. Comparing these three rates obtained for ground state ions, within their uncertainties, shows that the value of 2.2×10^{-7} cm^3 s^{-1} is the only value overlapped by all three sets of error bars. This therefore suggests that the correct value for the DR rate coefficient of ground state N_2^+ ions at 300 K is 2.2×10^{-7} cm^3 s^{-1}. This value is also in perfect agreement with the early FALP results of Mahdavi et al. [*Mahdavi et al.*, 1971]. Thus the temperature dependent rate coefficient for the DR of ground state N_2^+ ions is 2.2×10^{-7} $(T_e/300)^{-0.39}$ cm^3 s^{-1}.

[48] This conclusion is strengthened if we consider the results of two theoretical studies for v = 0 N_2^+. Both studies employed multichannel quantum defect theory calculations (MQDT). MQDT is a powerful technique that allows multiple electronic and vibrational states to be accounted for in the calculations. The first study we consider yielded a rate of $1.6 \times 10^{-7}(T_e/300)^{-0.37}$ cm^3 s^{-1}, which is in fair agreement with the observed rates for ground state ions [*Guberman*, 1993]. The second study yielded a rate of $2.1 \times 10^{-7}(T_e/300)^{-0.20}$ cm^3 s^{-1} around 300 K [*Guberman*, 2003]. The primary difference between these two studies is that the former only accounted for a single dissociating state whereas the latter accounted for several dissociating states as well as excited core Rydberg states. The second value is in near perfect agreement with our recommenda-

tions for the 300 K ground state rate, thus illustrating the significant recent improvements in the theoretical study of DR. It is conceivable that future improvements to theory will result in successful comparisons between theory and experiment over all temperatures.

[49] At this point we should issue a note of caution about the temperature dependences of rates. Mehr and Biondi quote a single temperature dependent rate for the entire range of 300–5000 K. It is unlikely that a single exponent accurately represents this entire temperature range. This is evidenced by the fact that we found it necessary to use separate fits for $T < 1200$ K and $T > 1200$ K for both the single pass and multipass N_2^+ rates. Even over these smaller temperature ranges, a single exponent may better represent some temperatures than others. This argument extends to all temperature dependent reaction rates, not just DR rates discussed here, and so care must always be exercised in the use of reaction rates.

[50] Although we are unable to resolve the rate coefficients for the individual vibrational states, we can nevertheless make some observations of the effects of vibrational excitation on the DR of N_2^+. The results of both single pass and multipass merged beams experiments indicate that the presence of $v > 0$ states leads to a reduction in the observed rate coefficient. In both cases we calculated an observed temperature dependent rate coefficient of $1.5 \times 10^{-7} (T_e/300)^{-0.39}$ cm^3 s^{-1}. This represents a 38% difference from the $v = 0$ value observed by all three of the afterglow groups. More significantly, since the CRYRING group was able to experimentally determine that their ion population consisted approximately of 50% ions with $v = 0$ and 50% ions with $v > 0$, the merged beams rate coefficients imply that a population entirely of $v > 0$ N_2^+ ions will have a temperature dependent rate coefficient of approximately $0.8 \times 10^{-7} (T_e/300)^{-0.39}$ cm^3 s^{-1}. This yields 2.8 as the ratio of the $v = 0$ to $v > 0$ rates at 300 K. It is evident that vibrational excitation has a significant impact on the DR of N_2^+ ions. These conclusions are consistent with the reanalysis of *Zipf*'s [1980a, 1980b] experiment [*Bates and Mitchell*, 1991].

[51] The controversial results of another merged beams study that require comment were omitted in the discussion above. In 1989, the results of a set of single pass experiments with N_2^+ ions were reported in which a special rf ion trap source was employed [*Noren et al.*, 1989]. By varying both the source pressure and the residence time in the source, the number of collisions an ion underwent could be manipulated prior to injection into the beam line. The intention was to enhance the collisional quenching of vibrationally excited ions. This group had successfully used this technique previously with H_2^+ [*Hus et al.*, 1988a; *Van der Donk et al.*, 1991] and with H_3^+ [*Hus et al.*, 1988a] to produce vibrational cool ions.

[52] The first set of N_2^+ data from *Noren et al.* [1989], reportedly corresponding to the hottest ions, was nearly identical to the original MEIBE results of *Mul and McGowan* [1979], to the new MEIBE results we have presented in this paper, and to the CRYRING results of *Peterson et al.* [1998]. By manipulating the source conditions, they produced two additional sets of data, each reportedly with subsequently vibrationally cooler ions. Their results seemed to indicate that as the ions were cooled vibrationally, the DR cross section decreased. Although these results were consistent with H_2^+ and H_3^+ results, this trend is opposite to the behavior demonstrated in Figure 4 and the above discussion. Of greater concern is the fact that if interpreted correctly, these results imply a $v = 0$ rate of $0.4 \times 10^{-7} (T_e/300)^{-0.39}$ cm^3 s^{-1}, a factor of 5 smaller than any other reported $v = 0$ value.

[53] The results of *Noren et al.* [1989] have continued to be a mystery to this day. In light of our discussion, it does not seem reasonable to attribute their observations to an experimental or calibration error. It is more likely that their observations are the result of some physical process reducing the cross sections as the ion collision rate in the source increases. A clue to the interpretation of these enigmatic results may come from our above discussion of the N_2^+ rates. Our discussion indicates that this unusually low rate cannot be due to $v = 0$ ions so that the original interpretation should be revisited. It is important to realize that the process represented in equation (16) is efficient in both directions. Not only is this process effective at collisionally quenching vibrationally excited ions, it can also be efficient at collisionally exciting vibrationally cool ions. This is not a concern in FALP experiments where the number density is high enough to effectively eliminate the vibrational reactivation of collisionally cooled ions. In an rf source, however, where the number density is much lower, it is conceivable that given enough collisions the ions will become vibrationally reactivated. The controversial value of $0.4 \times 10^{-7} (T_e/300)^{-0.39}$ cm^3 s^{-1} is comparable to the value of $0.8 \times 10^{-7} (T_e/300)^{-0.39}$ cm^3 s^{-1} that we calculated for $v > 0$ ions. A possible explanation of the results of *Noren et al.* [1989] is that as reported, the vibrational population of the ions varied as the source conditions were changed, but owing to vibrational reactivation the vibrational excitation increased rather than decreased. With this interpretation, the observations of *Noren et al.* [1989] become consistent with the body of results found in Table 2.

[54] We have extended our study of DR rates to the highest electron temperatures for which we believe the rates to be reliable. A comparison (see equation (13)) of f(v) versus the product $\sigma v f(v)$ for both the single pass MEIBE results and the CRYRING multipass results suggested that rate coefficients can be reliably calculated up to 4000 K for both merged beams N_2^+ experiments. These high temperature rates are given in Figure 7 and Table 4. *Mehr and Biondi* [1969] obtained their rate for the entire range of $300 \text{ K} \leq Te \leq 5000$ K so this also is included. The $v = 0$ rate for $T_e < 1200$ K is extrapolated to 5000 K and included in Figure 7 for comparison purposes. Since Mehr and Biondi worked with ground state ions and noticed no changes in the rate over this temperature range, this extrapolation seems to be a reasonably safe representation of the ground state rate at higher temperatures as well.

[55] It is immediately apparent from Figure 7 that vibrational excitation plays an increasingly significant role as T_e increases. A steeper $T_e^{-0.56}$ temperature dependence is observed for the vibrationally excited ions in the merged beams experiments. As a consequence, at 4000 K the rate coefficient for the mixed population ions of 0.44×10^{-7} cm^3 s^{-1} is smaller than the $v = 0$ value of 0.80×10^{-7} cm^3 s^{-1} by approximately a factor of 2. Again considering the fact that the CRYRING ion population

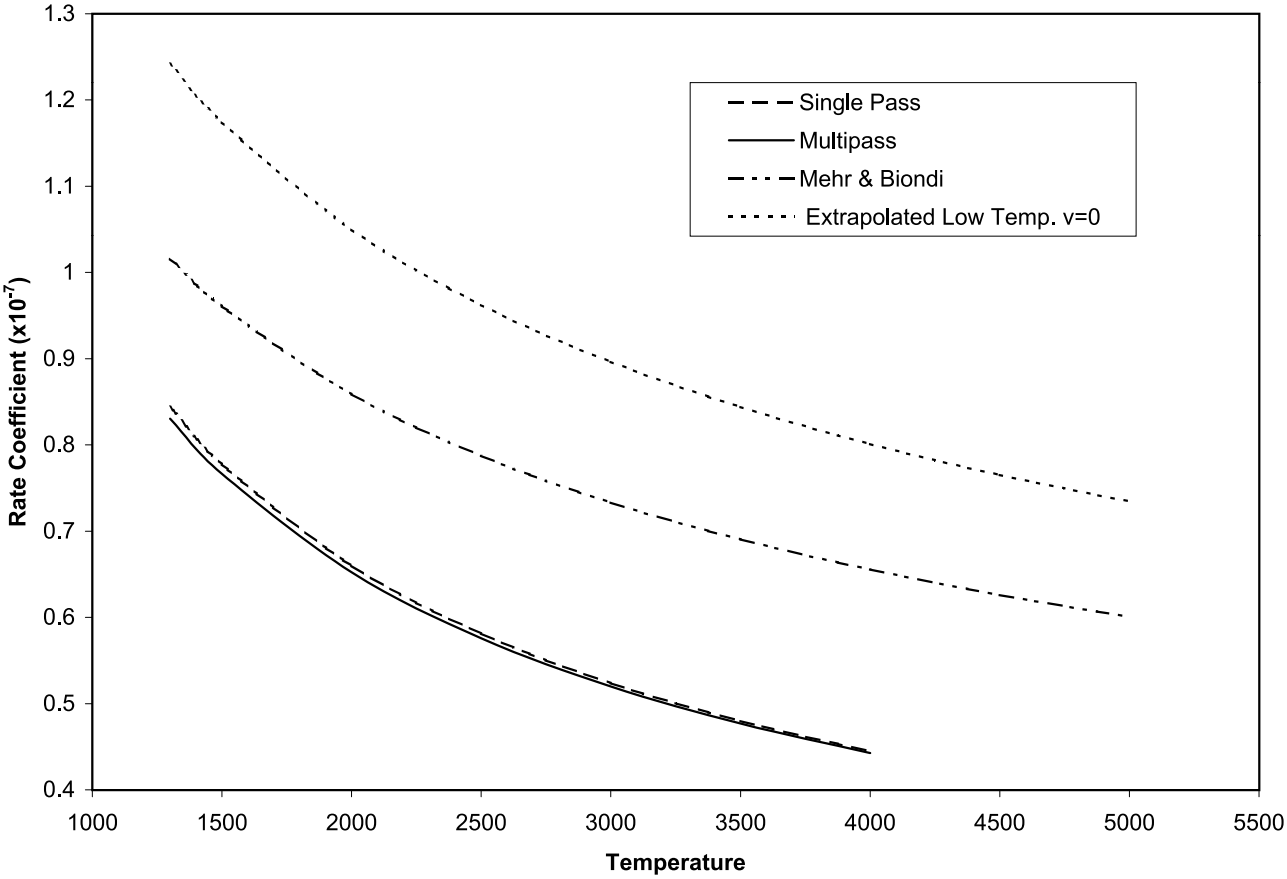

Figure 7. Rate coefficients for the dissociative recombination of N_2^+ for $T_e > 1200$ K.

was known to consist approximately of 50% ions with v = 0 and 50% ions with v > 0, this implies the very low rate of 0.08×10^{-7} cm^3 s^{-1} for a population entirely of v > 0 N_2^+ ions. By 4000 K, the DR rate for v > 0 ions is smaller than the rate for v = 0 by approximately a factor of 10. We will discuss implications of these results for ionospheric studies following our presentation of the O_2^+ and NO^+ results.

3.3. Dissociative Recombination of O_2^+

[56] The relevant rate coefficients for the DR of O_2^+ for $T_e < 1200$ K are presented in Figure 8 and Table 5. As with N_2^+, we start with the analysis of the low temperature rates, followed by a discussion of rates for higher temperatures.

[57] Since our O_2^+ ions were produced by the electron impact ionization of O_2, we expect the vibrational levels to have been initially populated according to the Frank-Condon distribution as in the N_2^+ case. For this beam, we observed a temperature dependent rate coefficient of $0.90 \times 10^{-7}(T_e/300)^{-0.49}$ cm^3 s^{-1}.

[58] The multipass O_2^+ results were obtained at the CRYRING facility in Stockholm [*Peverall et al.*, 2001]. As with their N_2^+ experiment, the hollow cathode ion source was used to maximize vibrational cooling. A careful analysis of their DR products indicated that the beam of O_2^+ ions was predominantly in the v = 0 state. The observed rate coefficient for these ground state ions was $2.4 \times 10^{-7}(T_e/300)^{-0.70}$ cm^3 s^{-1}. In addition to measuring the rate coefficient for ground state ions, this group was able to experimentally determine the branching ratios of the DR products for O_2^+ ions in the ground electronic and vibrational state.

[59] *Mehr and Biondi* [1969] obtained results using the microwave afterglow apparatus described above. The DR rate coefficient they obtained for O_2^+ for $T_e < 1200$ K was $1.95 \times 10^{-7}(T_e/300)^{-0.70}$ cm^3 s^{-1}. As was the case with their N_2^+ experiment, the ions were in the v = 0 state. By using a high purity neon buffer gas, they were able to avoid the problem of contamination with complex ions that they had encountered with N_2^+. Mehr and Biondi expressed concern, however, that this procedure would lead to the production of some O_2^+ ions in the excited metastable $a^4\Pi_u$ state. Comparisons with earlier results indicated that any effects of such contamination on their results were negligible. This however remains a valid concern that needs to be addressed for all O_2^+ DR experiments.

[60] As part of a FALP study of the DR of NO^+, the DR rate coefficient for O_2^+ at $T_e = 300$ K was determined to be 1.9×10^{-7} cm^3 s^{-1} [*Mostefaoui et al.*, 1999]. The O_2^+ ions were formed when N_2 and O_2 were used as the parent gases

Table 4. High-Temperature N_2^+ DR Rate Coefficients

Source	Rate Coefficient, cm^{3}s^{-1}	Temperature Range, K
Multipass	$(1.95 \pm 0.29) \times 10^{-7}(T_e/300)^{-0.57}$	1200 < Te < 4000
Single Pass	$(1.88 \pm 0.28) \times 10^{-7}(T_e/300)^{-0.56}$	1200 < Te < 4000
Mehr and Biondi	$(1.8 \pm 0.4) \times 10^{-7}(T_e/300)^{-0.39}$	300 < Te < 5000

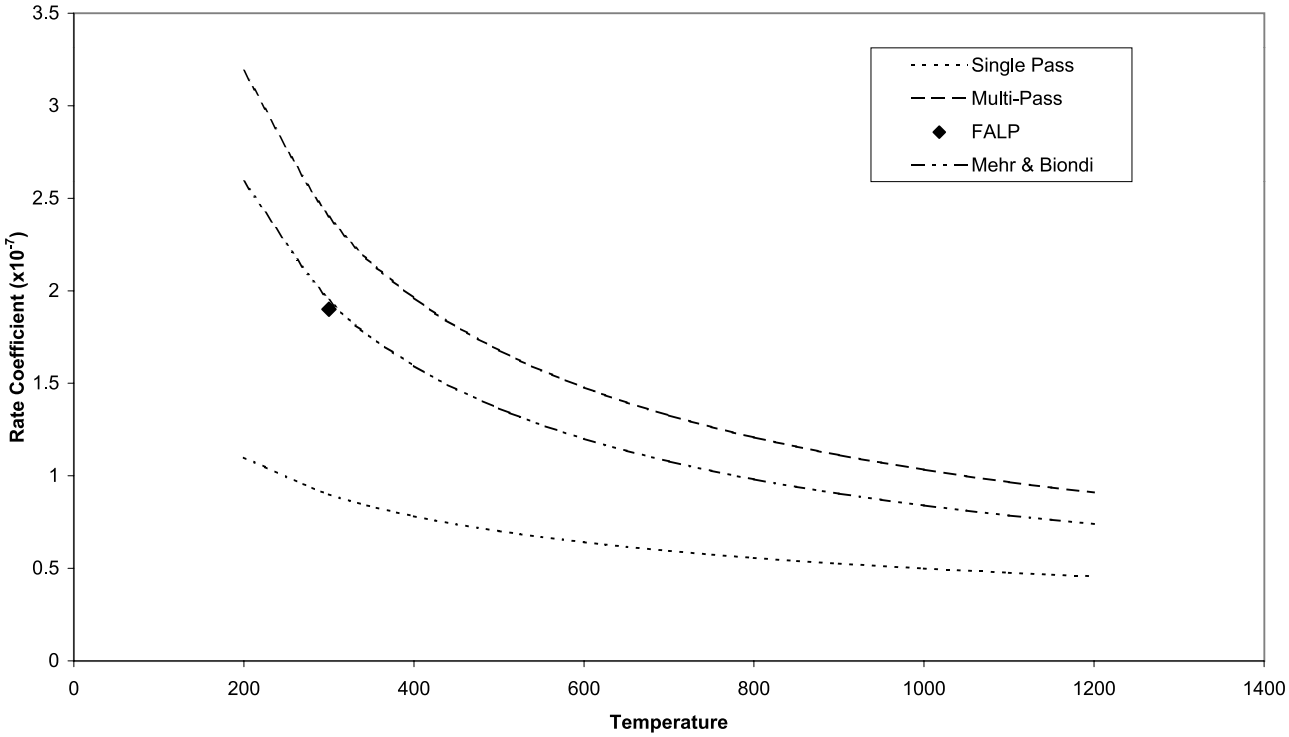

Figure 8. Rate coefficients for the dissociative recombination of O_2^+ for $T_e < 1200$ K.

for the production of NO^+. In this particular experiment, the O_2^+ was formed through the reaction

$$N^+ + O_2 \rightarrow O_2^+ + N. \quad (17)$$

As a result, the O_2^+ ions were exclusively formed in the $X^2\Pi_g$ ground electronic state with v = 0–2 levels populated. Therefore contamination by ions in metastable states was not a concern in this FALP experiment. The v = 1–2 levels would have been subsequently collisionally quenched, leaving O_2^+ ions in the ground electronic and vibrational levels. This same rate was observed in the FALP results of *Mahdavi et al.* [1971].

[61] Since the $a^4\Pi_u$ state has an approximate lifetime of 0.1 s [*Kella et al.*, 1997], it also would not have been present in the multipass experiment due to beam circulation times. Thus the multipass rate is understood to reflect a beam of ions in the ground electronic and vibrational state.

[62] Figure 9 compares the four experimental rates just described at 300 K. The three experiments involving ground state ions all agree well within experimental uncertainties. This, in combination with Figure 8, confirms that for $T_e <$ 1200 K the DR rate coefficient for O_2^+ ions in the ground electronic and vibrational states is given by the generally accepted value of $1.95 \times 10^{-7}(T_e/300)^{-0.70}$ cm^3 s^{-1}. In light of this discussion, Figure 8 demonstrates that vibrational excitation plays a more significant role in the DR of O_2^+ than of N_2^+. This is particularly true at the lower end of the temperature scale. At 300 K, the vibrationally excited ions of our single pass experiment yielded an observed rate coefficient smaller than the ground state value by a factor of 2.2. The less steep temperature dependence of the vibrationally excited ions causes the difference in observed rates to decrease as the temperature increases towards 1200 K. Nevertheless, even at 1200 K the percent difference between the rate for ground state ions and the rate for vibrationally excited ions is nearly 70%.

[63] The relatively long lifetime of the $a^4\Pi_u$ state in comparison to the short ion transit time in MEIBE experiments renders it likely that this state was populated to some extent in our experiment. The excellent agreement between the results of *Mehr and Biondi* [1969] and those of the recent FALP and storage ring experiments, however, demonstrates that contamination with $a^4\Pi_u$ ions does not significantly affect the observed DR rates. From this we infer that the recombination rate for the $a^4\Pi_u$ state is nearly identical to the value quoted above for ions in the ground electronic and vibrational state. It follows then that our low rate is due to the presence of vibrationally excited ions in the ground electronic state.

[64] The high temperature DR rate coefficients for O_2^+ are given in Figure 10 and Table 6. Using the process outlined above for N_2^+, we determined that the rate coefficient could be reliably calculated for our single pass experiment up to 4000 K. For the multipass experiment [*Peverall et al.*, 2001] we determined that the rates could be reliably calculated up to 5000 K. Since *Peverall et al.* [2001] only calculated rates up to 1000 K, we used their cross sections to calculate multipass rates up to 5000 K. This is the multipass value found in Table 6 and Figure 10.

Table 5. O_2^+ DR Rate Coefficients ($T_e < 1200$ K)

Source	Rate Coefficient, cm^3s^{-1}
Single Pass	$(0.90 \pm 0.14) \times 10^{-7}(T_e/300)^{-0.49}$
Multipass	$(2.4 \pm 0.36) \times 10^{-7}(T_e/300)^{-0.70}$
Mehr and Biondi	$(1.95 \pm 0.2) \times 10^{-7}(T_e/300)^{-0.70}$
FALP	1.9×10^{-7} at T = 300 K

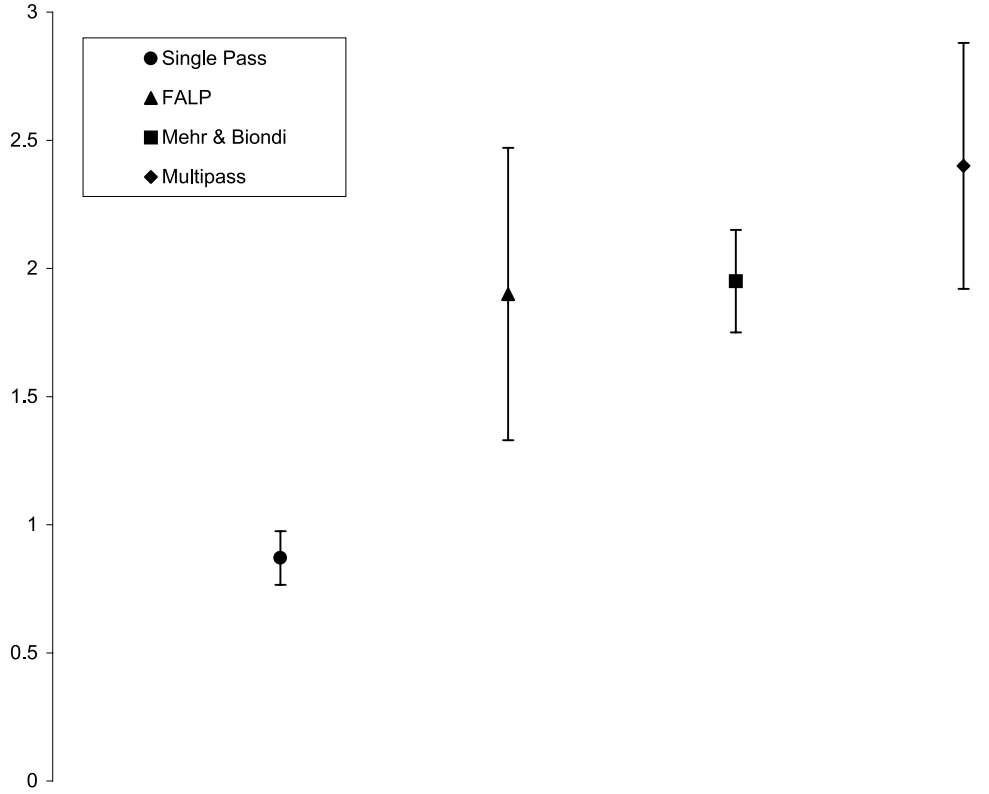

Figure 9. Experimental rate coefficients for the dissociative recombination of O_2^+ at T_e = 300 K.

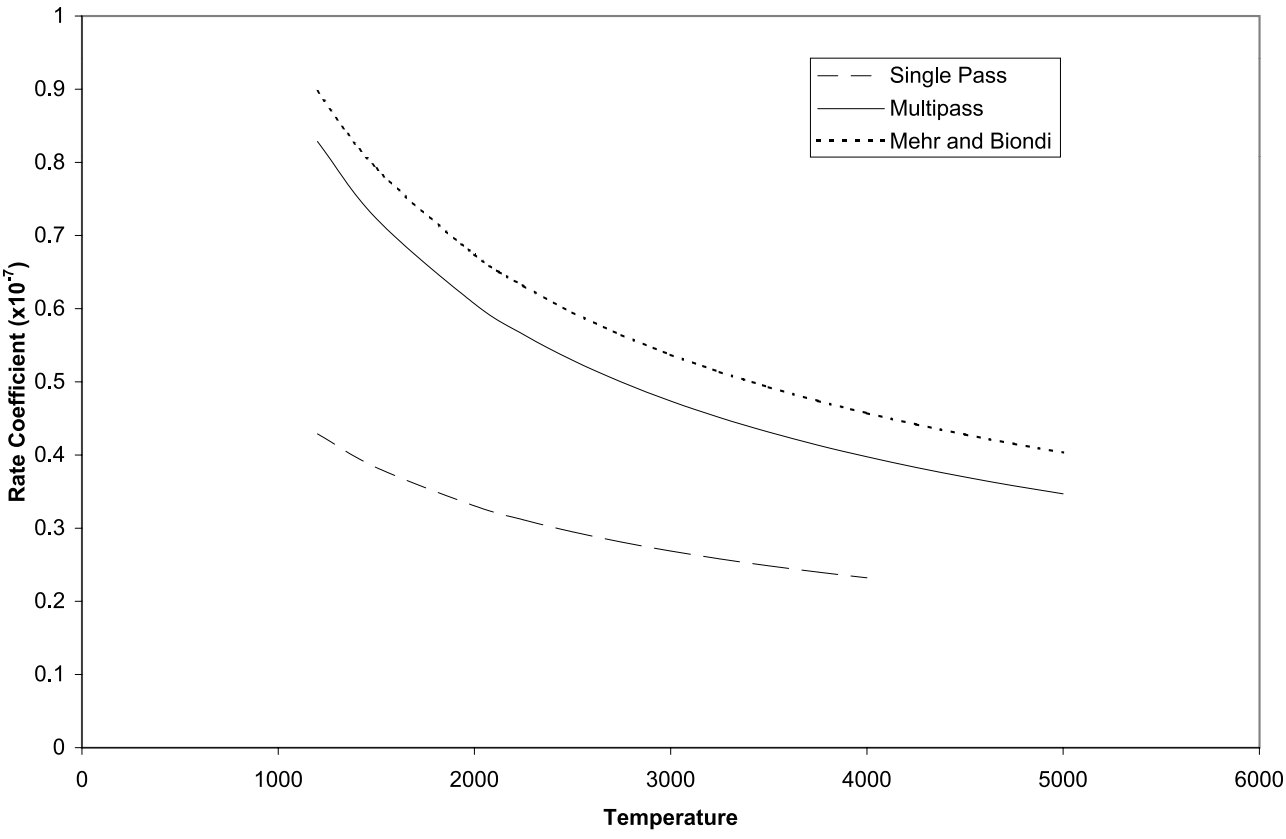

Figure 10. Rate coefficients for the dissociative recombination of O_2^+ for T_e > 1200 K.

Table 6. High-Temperature O_2^+ DR Rate Coefficients

Source	Rate Coefficient, cm^3s^{-1}	Temperature Range, K
Multipass	$(1.93 \pm 0.29) \times 10^{-7}(T_e/300)^{-0.61}$	$1200 < Te < 5000$
Single Pass	$(0.90 \pm 0.14) \times 10^{-7}(T_e/300)^{-0.51}$	$1200 < Te < 4000$
Mehr and Biondi	$(1.95 \pm 0.2) \times 10^{-7}(T_e/300)^{-0.56}$	$1200 < Te < 5000$

[65] There are several things to notice about the high temperature results. First, the observed temperature dependence for the multipass experiment changes from $T_e^{-0.7}$ below 1200 K to $T_e^{-0.6}$ above 1200 K. Above 1200 K our calculated multipass rates are almost identical to those of *Mehr and Biondi* [1969]. In Figure 10, the small divergence between these two rates is due to the slight difference in temperature dependence. This divergence is well within the experimental uncertainties and so the agreement can be considered excellent.

[66] The second thing to notice is that both the ground state ions and the vibrationally excited ions have essentially the same temperature dependence at higher temperatures. Thus the rate for excited ions is lower than the ground state rate by approximately a factor of 2 over the entire range of 200 K up to 4000 K. We will discuss implications of these results to ionospheric studies following our presentation of the NO^+ results.

3.4. Dissociative Recombination of NO^+

[67] The relevant rate coefficients for the DR of NO^+ for $T_e < 1200$ K are found in Figure 11 and Table 7. By varying the ion production chemistry, a recent FALP study of the DR of NO^+ observed that vibrational excitation has a significant impact on the observed recombination rates for this molecular species [*Mostefaoui et al.*, 1999]. They achieved a population of ions in the ground electronic and vibrational state through the use of an NO parent gas. NO^+ was produced by charge exchange reactions between the parent NO and Ar^+ ions in the flow. Initially, at least 85% of the NO^+ would have been in the excited metastable $a^3\Sigma^+$ state with the remaining 15% being in the $X^1\Sigma^+$ ground state. This excited metastable state is long-lived, since its transition to the ground state requires a spin-forbidden triplet-singlet transition. Since, however, the NO parent gas is paramagnetic, it very efficiently induces the quenching triplet-singlet transition [*Chiu*, 1972]. The combination of the high reaction rate for this induced transition and the high number density of NO molecules ensures the rapid quenching of the NO^+ to the $X^1\Sigma^+$ ground state. Calculations indicate that for this experiment the vibrational deactivation time for the NO^+ by collisions with NO was 20 μs [*Mostefaoui et al.*, 1999]. This is much less than the 500 μs hydrodynamic flow time of ions in the FALP system, and thus the reported rate of $(3.9 \pm 1.0) \times 10^{-7}$ cm^3s^{-1} at 300 K corresponds to NO^+ ions in the ground electronic and vibrational state [*Mostefaoui et al.*, 1999].

Table 7. NO^+ DR Rate Coefficients ($T_e < 1200$ K)

Source	Rate Coefficient, cm^3s^{-1}
Single Pass	$(1.0 \pm 0.2) \times 10^{-7}(T_e/300)^{-0.48}$
Multipass (Reported)	$(4.0 \pm 2.0) \times 10^{-7}$ at T = 300 K
Multipass (Calculated Here)	$(3.5 \pm 0.5) \times 10^{-7}(T_e/300)^{-0.69}$
FALP (Ground State)	$(3.9 \pm 1.0) \times 10^{-7}$ at T = 300 K
FALP (Excited)	$(1.6 \pm 0.5) \times 10^{-7}$ at T = 300 K
MQDT	3.7×10^{-7} $(T_e/300)^{-0.6}$

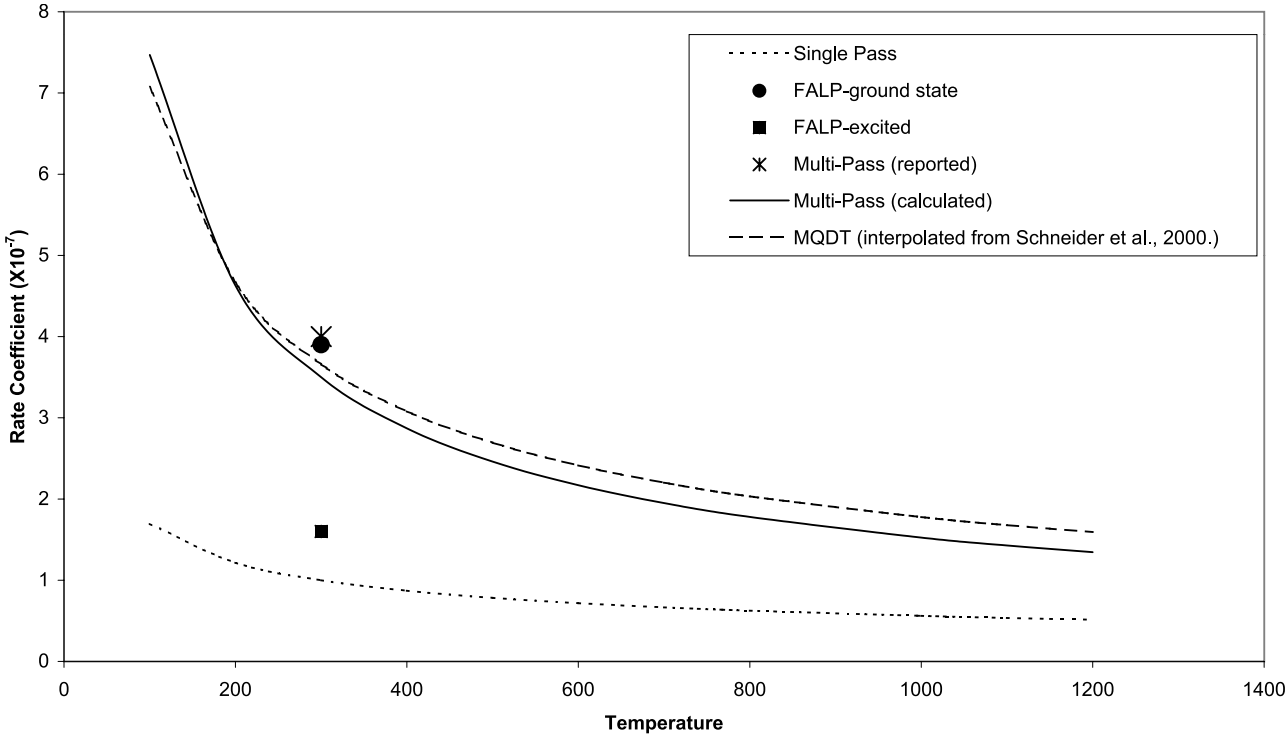

Figure 11. Rate coefficients for the dissociative recombination of NO^+ for $T_e < 1200$ K.

Table 8. Population of Vibrational States of NO^+ Produced by $N^+ + O_2$

Vibrational State	Population
0	0.03
1	0.05
2	0.07
3	0.08
4	0.11
5	0.12
6	0.14
7	0.17
8	0.07
9	<0.01
10	0.02
11	0.06
12	0.07
13	0.04
14	<0.01

[68] The same group repeated their study with a mixed parent gas of N_2 and O_2, in place of the NO [*Mostefaoui et al.*, 1999]. The NO^+ production mechanisms in this case are

$$N^+ + O_2 \rightarrow NO^+ + O \tag{18}$$

and

$$O^+ + N_2 \rightarrow NO^+ + N. \tag{19}$$

[69] Although reaction (19) produces NO^+ ions which are in the ground electronic and vibrational state, the reaction rate at room temperature is so slow that this process can be ignored. The process in reaction (18), with a much higher rate, is therefore the mechanism responsible for the NO^+ production in this second experiment. Reaction (18) is known to produce NO^+ ions in the ground electronic state. In fact, less than 2% of the ions produced by reaction (18) are in the $a^3\Sigma^+$ state. The ions produced through reaction (18) are formed in an array of vibrational states populated according to Table 8 [*Mostefaoui et al.*, 1999]. Both theoretical and experimental studies show that the first five vibrational levels of the $X^1\Sigma^+$ ground state of NO^+ have lifetimes in the range of 20–90 ms, which is significantly longer than the hydrodyamic time in the FALP experiment of *Mostefaoui et al.* [1999]. Since neither N_2 nor O_2 efficiently vibrationally deactivate NO^+, the ions would have retained the same vibrational population throughout the entire experiment. Therefore the rate of $(1.6 \pm 0.5) \times 10^{-7}$ cm^3 s^{-1} at 300 K obtained by *Mostefaoui et al.* [1999] for a mixed N_2 and O_2 source is understood to reflect the vibrational population distribution of Table 8.

[70] Our single pass NO^+ experiments used a source gas consisting of 50% N_2 and 50% O_2. The dominant NO^+ production mechanism in our source therefore should also have been reaction (18). Given the 10^{-4} s production to interaction times for MEIBE ions, and in light of the above discussion of the FALP results, it follows that our observed rate of $(1.0 \pm 0.2) \times 10^{-7}(T_e/300)^{-0.48}$ cm^3 s^{-1} also should be understood to reflect the vibrational population distribution of Table 8. Our single pass rate agrees with the FALP rate, within the uncertainties, which is not surprising considering both experiments should have had very similar vibrational population distributions.

[71] The storage ring group in Aarhus, Denmark performed multipass measurements of cross sections for the DR of NO^+ [*Vejby-Christensen et al.*, 1998]. Their NO^+ ions were produced from an NO parent gas, and the experiment was performed with two different ion sources. On the basis of the above discussion, the ions would probably have been produced in both the metastable $a^3\Sigma^+$ state and the $X^1\Sigma^+$ ground state, with a variety of vibrational levels populated. Since, however, the longest lived excited state that may have been present, $a^3\Sigma^+(v = 0)$, has a lifetime of 720 ± 70 ms, storing the beam for several seconds prior to injection would have been adequate to achieve a beam of $X^1\Sigma^+(v = 0)$ ions [*Vejby-Christensen et al.*, 1998]. From a combination of a direct measurement of the absolute rate coefficient at zero energy and the energy dependence of the DR cross-sections, the Arhus group inferred a rate at 300 K of 4×10^{-7} cm^3 s^{-1}. Unfortunately, their zero energy recombination rate had an uncertainty of ±50% due to a weak beam current and so the inferred rate at 300 K will be equally uncertain, making meaningful comparisons difficult.

[72] For the sake of obtaining a temperature dependent rate coefficient for ground state NO^+ ions, we integrated the energy-dependent multipass cross sections of *Vejby-Christensen et al.* [1998] using equations (13), (14), and (15) as discussed earlier in our paper. This yielded a rate of $(3.5 \pm 0.5) \times 10^{-7}(T_e/300)^{-0.69}$ cm^3 s^{-1} for the multipass experiment with ground state NO^+. The uncertainty in the rate was estimated by assuming a somewhat typical systematic uncertainty of ±20% in the cross sections over the entire energy range. This calculated rate is in excellent agreement with the 300 K rate observed for ground state NO^+ in the FALP experiment of *Mostefaoui et al.* [1999] discussed above, with the FALP results of *Mahdavi et al.* [1971], and with the recent MQDT calculation of 3.7×10^{-7} $(T_e/300)^{-0.6}$ cm^3 s^{-1} for NO^+ ions in the $X^1\Sigma^+(v = 0)$ state [*Schneider et al.*, 2000, Figure 7].

[73] It is interesting to note that the two NO^+ beams obtained with the two different ion sources in this multipass study had different rotational temperatures, kT = 75 meV and kT = 150 meV. These rotational temperature differences yielded no statistically significant difference in the results. This suggests that the DR of NO^+ is independent of the initial rotational state [*Vejby-Christensen et al.*, 1998].

[74] The preceding discussion, coupled with Figure 12, shows that the various theoretical and experimental results for $X^1\Sigma^+(v = 0)$ NO^+ ions are in excellent agreement with each other. This also demonstrates the significant effect that vibrational excitation has on the DR of NO^+. The two sets of experimental results for $X^1\Sigma^+(v > 0)$ are in good agreement with each other and yet clearly distinct from the ground state results (see Figure 12). Since only 3% of the ions in the studies with excited NO^+ (see Table 8) were in the v = 0 level, this allows an effective comparison of rates for v = 0 with v > 0. The ratio of the 300 K rates for v = 0 to v > 0 ions is approximately 3, very similar to the ratio of 2.8 observed above for N_2^+.

[75] It is important to note that while vibrational excitation plays a significant role in the recombination rate for NO^+, consistent with theoretical predictions and earlier

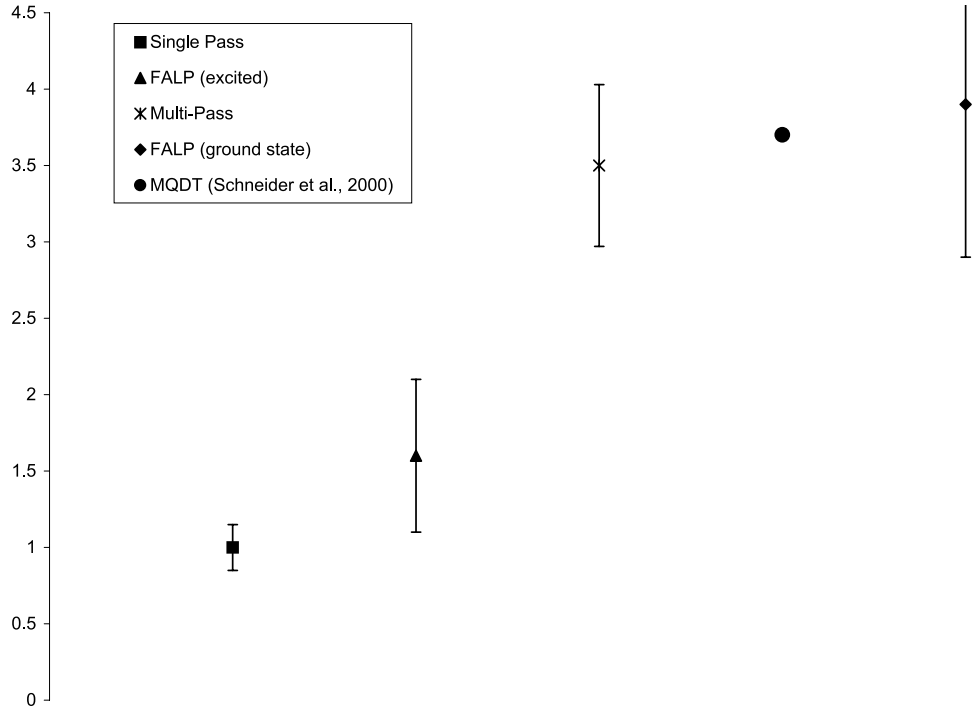

Figure 12. Rate coefficients for the dissociative recombination of NO^+ at T_e = 300 K.

experiments [*Mostefaoui et al.*, 1999], it does not change the primary product channel. From the potential curves (see, for example, *Vejby-Christensen et al.* [1998, Figure 1] or *Schneider et al.* [2000, Figures 1 and 2]) we see that for v = 0, the $B^2\Pi$ state is the most important neutral dissociating state. This state dissociates to $N(^2D) + O(^3P)$ [*Mostefaoui et al.*, 1999]. For v > 0, the $L^2\Pi$, $A'(^2\Sigma^+)$, and $I^2\Sigma^+$ states appear to be the most significant neutral dissociating states. The respective product channels of these three states are $N(^2D) + O(^3P)$, $N(^4S) + O(^3P)$, and $N(^4S) + O(^1D)$ [*Vejby-Christensen et al.*, 1998]. Calculations, however, show that the $^2\Sigma^+$ states make no effective contribution to the DR cross-section at low energies, and even at higher energies they never dominate. Their largest combined contribution is at an electron energy of 4 eV where they contribute 30% of the total cross section [*Schneider et al.*, 2000]. Thus the $L^2\Pi$ state is most significant dissociative neutral state for v > 0. Since this state dissociates to the same products as the $B^2\Pi$ state through which the v = 0 ions dissociate, then both v = 0 and v > 0 ions will primarily dissociate to $N(^2D) + O(^3P)$. The only observations of branching ratios in the DR of NO^+ have been with v = 0 ions and the results are consistent with this analysis [*Vejby-Christensen et al.*, 1998].

[76] The high-temperature DR rate coefficients for NO^+ are given in Figure 13 and Table 9. Using the process outlined above for N_2^+, we determined that the rate coefficient could be reliably calculated for the single pass experiment up to 4000 K. For the multipass experiment [*Peverall et al.*, 2001] we have calculated the rates up to 5000 K, although the fact that they measured cross sections for electron energies up to 30 eV suggests this rate might reasonably be extended up to 10,000 K.

[77] We can see from Figure 13 that the ratio of DR rates at high temperatures for v = 0 ions to v > 0 ions remains around 3, as was the case for lower temperatures. The energy dependence however has noticeably changed from the low temperature values. Interestingly, at higher temperatures both v = 0 and v > 0 NO^+ DR rates have a temperature dependence of $T_e^{-0.6}$. This is very similar to what we noted for O_2^+.

4. Summary and Conclusions

[78] Our goal in this paper, besides reviewing the latest advances in the study of DR for the space community, has been to try to make sense of the potentially bewildering array of published recombination rates. We have done so by analyzing the physical and chemical conditions present during the various experimental determinations of recombination rates in light of what molecular physics tells us about the various species of interest. From this it is evident that the initial ionic state plays a large role in the DR process for the species of ions discussed in this paper. Vibrationally excited ions produce an observed DR rate coefficient that is significantly different from that observed for ground state ions for each species of ions considered here. This also holds true for the methane family of ions which we have discussed in detail elsewhere [*Sheehan and St.-Maurice*, 2004].

[79] To summarize, based on the analysis presented above, for N_2^+ and $T_e < 1200$ K, we conclude that for v = 0 of the ground electronic state, the rate is $2.2 \times 10^{-7} (T_e/300)^{-0.39}$ cm^3 s^{-1}, while for v > 0 it is $0.8 \times 10^{-7} (T_e/300)^{-0.39}$ cm^3 s^{-1}. For O_2^+ and $T_e < 1200$ K, we conclude that for v = 0 of the ground electronic state, the rate is $1.95 \times 10^{-7}(T_e/300)^{-0.70}$ cm^3 s^{-1}, while for the vibrationally excited ions it is $0.90 \times 10^{-7}(T_e/300)^{-0.49}$ cm^3 s^{-1}. We have also been able to infer that this rate observed for O_2^+ ions in the ground electronic and vibrational state reflects the recombination rate for the $a^4\Pi_u$ state. For NO^+ and $T_e <$

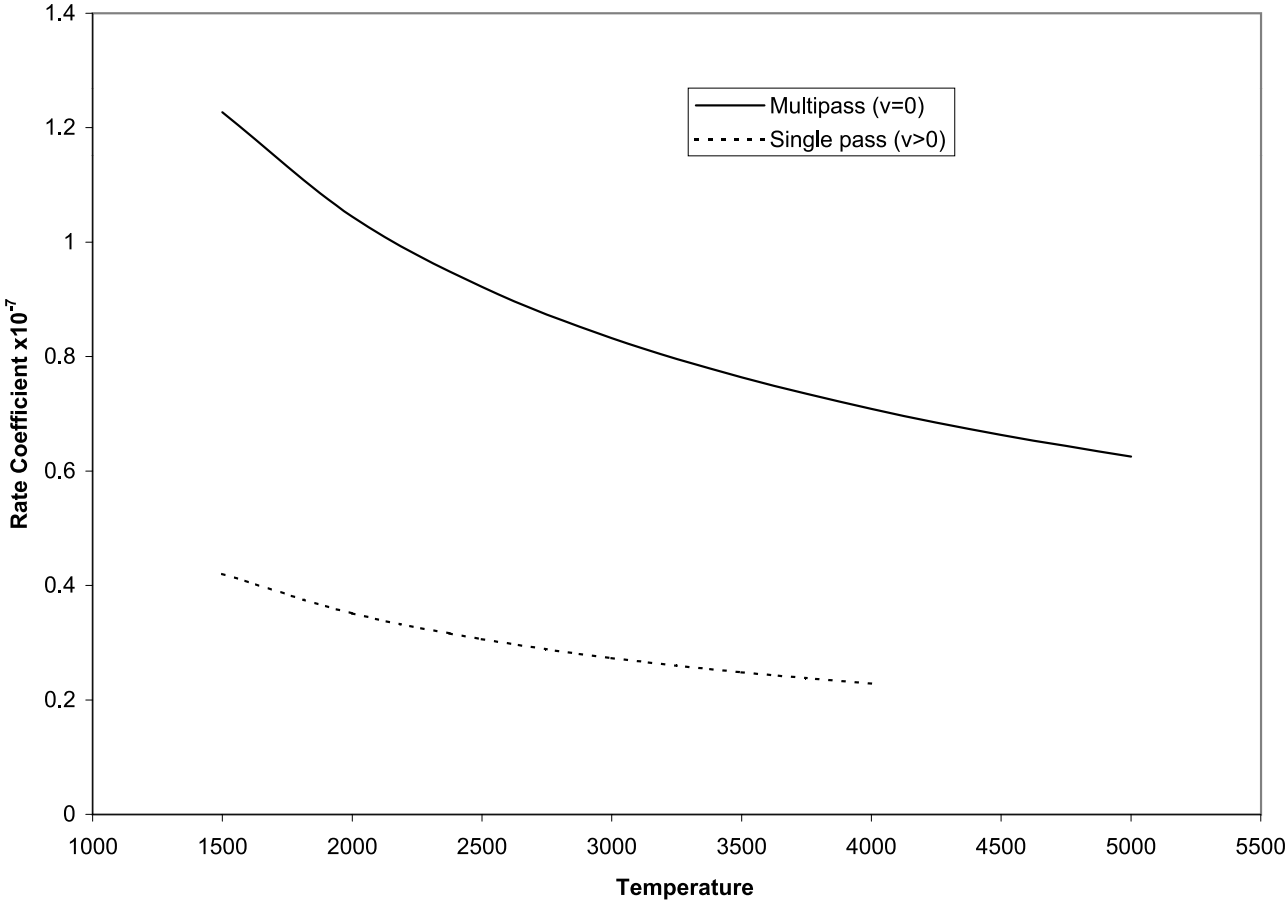

Figure 13. Rate coefficients for the dissociative recombination of NO^+ for $T_e > 1200$ K.

1200 K, we conclude that for v = 0 the rate is $3.5 \times 10^{-7}(T_e/300)^{-0.69}$ cm^3 s^{-1} with no observed dependence on rotational temperature, while for v > 0 the rate is $1.0 \times 10^{-7}(T_e/300)^{-0.48}$ cm^3 s^{-1}. It is also noted that for NO^+, vibrational excitation does not alter the dissociation product channels.

[80] The two most obvious remaining difficulties are that we were unable to resolve rates for individual vibrational states and that the population distribution of vibrational states for ionospheric ions is difficult if not impossible to determine. This makes it clear that one must be cautious in their treatment of DR in the ionosphere. In spite of these remaining difficulties, this analysis brings us closer to a realistic understanding of DR in the ionosphere. We have intentionally included as many details in our analysis as possible to allow others to draw their own conclusions regarding the applications of our results to specific ionospheric studies. We will only make a few general and speculative comments here concerning applications.

[81] To obtain an estimate of the distribution of vibrational states for a given species of ion under a given set of ionospheric conditions, the main sources and sinks of excited ions need to be considered. Chemical processes such as reactions (16)–(19) are one source of vibrationally excited ions. The electron impact excitation of cold ions is another source of vibrationally excited ions. The electron impact ionization of the parent neutrals also needs to be considered, particularly during energetic electron precipitation such as in the aurora. As discussed above, the latter is known to result in a Frank-Condon distribution of vibrational states. For heteronuclear ions the primary sink is radiative deactivation, although in light of the earlier discussion of vibrational lifetimes this mechanism is likely insignificant for homonuclear diatomic ions. Collisional quenching is another sink that must be considered. The net effect of all of these sources and sinks will likely vary considerably as changing ionospheric conditions cause the individual mechanisms to become more or less significant.

[82] A first-order estimate of ionospheric vibrational population distributions could potentially be obtained by using the DR rate coefficient as a free parameter in models or the analysis of observations. The rates discussed above might serve as the limiting values on this parameter. The rate value that reproduces observed ionospheric conditions would then give an indication of the percentage of ions in vibrationally excited states. For instance, during times when electron production and loss is well known, correlations between observed electron number densities and temper-

Table 9. High-Temperature NO^+ DR Rate Coefficients

Source	Rate Coefficient, cm^3s^{-1}	Temperature Range, K
Multipass (v = 0)	$(3.02 \pm 0.45) \times 10^{-7}(T_e/300)^{-0.56}$	1200 < Te < 5000
Single Pass (v > 0)	$(1.14 \pm 0.17) \times 10^{-7}(T_e/300)^{-0.62}$	1200 < Te < 4000

atures [*St.-Maurice et al.*, 1999, Figure 4] can be used to determine the ionospheric rate coefficient. This rate can then be compared with the rates discussed here, and thus inferences about the ion populations can be made. Similarly, by comparing the conditions in the ionosphere at a given time with the ion source conditions discussed above, an appropriate rate can be selected for modeling or analysis purposes with more confidence.

[83] Since DR is an important source of excited neutral atoms, a decrease in the observed emissions by N and O could be an indicator of the presence of vibrationally excited ions. This is because the DR rates for all three species of ions discussed here decrease for vibrationally excited ions. Similarly, during periods of significant vibrational excitation there should be an observed enhancement in electron and ion densities.

[84] It is clear that a significant combination of observational and modeling work is necessary to determine the full effects of vibrationally excited molecular ions on the ionosphere. It is our hope that the work presented here will bring us one step closer to a fuller understanding of the ionosphere.

[85] **Acknowledgments.** This work has been partially supported through grants from the Canadian NSERC and through a Patterson Research Grant.

[86] Arthur Richmond thanks Vincent J. Abreu and another reviewer for their assistance in evaluating this paper.

References

Abreu, V. J., S. C. Solomon, W. E. Sharp, and P. B. Hays (1983), The dissociative recombination of O_2^+: The quantum yield of O (^{1}S) and O (^{1}D), *J. Geophys. Res.*, *88*, 4144–4149.

Alge, E., N. G. Adams, and D. Smith (1983), Measurement of the dissociative recombination coefficients of O_2^+, NO^+, and NH4$^+$ in the temperature range 200–600 K, *J. Phys. B At. Mol. Opt. Phys.*, *16*, 1433–1444.

Amitay, Z., D. Zajfman, and P. Forck (1994), Rotational and vibrational lifetime of isotopically asymmetrized homonuclear diatomic molecular ions, *Phys. Rev. A*, *50*, 2304–2308.

Amitay, Z., D. Zajfman, P. Forck, U. Hechtfischer, B. Seidel, M. Grieser, D. Habs, R. Repnow, D. Schwalm, and A. Wolf (1996), Dissociative recombination of CH^+: Cross sections and final states, *Phys. Rev. A*, *54*, 4032–4050.

Auerbach, D., R. Cacak, R. Caudano, T. D. Gaily, C. J. Keyser, J. Wm. McGowan, J. B. A. Mitchell, and S. F. J. Wilk (1977), Merged electron-ion beam experiments. I. Methods and measurements of (e-H_2^+) and (e-H_3^+) dissociative-recombination cross sections, *J. Phys. B At. Mol. Opt. Phys.*, *10*, 3797–3920.

Banks, P. M., and G. Kockarts (1973), *Aeronomy*, Academic, San Diego, Calif.

Bardsley, J. N. (1968), The theory of dissociative recombination, *J. Phys. B At. Mol. Opt. Phys.*, *1*, 365–380.

Bardsley, J. N. (1983), Dissociative recombination of electrons with NO^+ ions, *Planet. Space Sci.*, *31*, 667–670.

Bates, D. R., and J. B. A. Mitchell (1991), Rate coefficients for N_2^+ (v) dissociative recombination, *Planet. Space Sci.*, *39*, 1297–1300.

Brekke, A. (1997), *Physics of the Upper Polar Atmosphere*, John Wiley, Hoboken, N. J.

Canosa, A., J. C. Gomet, B. R. Rowe, and J. L. Queffelec (1991), Flowing Afterglow Langmuir Probe measurement of the N_2^+(v = 0) dissociative recombination rate coefficient, *J. Chem. Phys.*, *94*, 7150–7160.

Chiu, Y.-N. (1972), On singlet-triplet transitions induced by exchange with paramagnetic molecules and the intermolecular coupling of spin angular momenta, *J. Chem. Phys.*, *56*, 4882–4898.

Compton, R. N., and J. N. Bardsley (1984), Dissociation of molecules by slow electrons, in *Electron-Molecule Collisions*, edited by I. Shimamura and K. Takayanagi, pp. 275–349, Plenum, New York.

Cunningham, A. J., and R. M. Hobson (1972), Dissociative recombination at elevated temperatures. IV. N_2^+ dominated afterglows, *J. Phys. B At. Mol. Opt. Phys.*, *5*, 2328–2331.

Davidson, D. F., and R. M. Hobson (1987), The shock tube determination of the dissociative recombination rate of NO^+, *J. Phys. B At. Mol. Opt. Phys.*, *20*, 5753–5756.

Geoghegan, M., N. G. Adams, and D. Smith (1991), Determination of the electron-ion dissociative recombination coefficients for several molecular ions at 300 K, *J. Phys. B At. Mol. Opt. Phys.*, *24*, 2589–2599.

Guberman, S. L. (1987), The production of O (^{1}S) from dissociative recombination of O_2^+, *Nature*, *327*, 408–409.

Guberman, S. L. (1989). Ab initio studies of dissociative recombination, in *Dissociative Recombination: Theory, Experiment, and Applications*, edited by J. B. A. Mitchell and S. L. Guberman, p. 45, World Sci., River Edge, N. J.

Guberman, S. L. (1991), Dissociative recombination of the ground state of N_2^+, *Geophys. Res. Lett.*, *18*, 1051–1054.

Guberman, S. L. (1993), Electron-ion continuum-continuum mixing, in *Dissociative Recombination: Theory, Experiment, and Applications*, edited by B. Rowe, J. B. A. Mitchell, and A. Canosa, p. 47, Plenum, New York.

Guberman, S. L. (1997), Mechanism for the green glow of the upper atmosphere, *Science*, *278*, 1276–1278.

Guberman, S. L. (2003), The dissociative recombination of N_2^+, in *Dissociative Recombination of Molecular Ions with Electrons*, p. 187, Plenum, New York.

Guberman, S. L., and A. Giusti-Suzor (1991), The generation of O (^{1}S) from the dissociative recombination of O_2^+, *J. Chem. Phys.*, *95*, 2602–2613.

Gunton, R. C., and T. M. Shaw (1965), Electron-ion recombination in nitric oxide in the temperature range 196 to 358 K, *Phys. Rev.*, *140*, 194–200.

Huang, C. M., M. A. Biondi, and R. Johnsen (1975), Variation of electron-NO^+-ion recombination coefficient with electron temperature, *Phys. Rev. A*, *11*, A756–A763.

Hus, H., F. Yousif, C. Noren, A. Sen, and J. B. A. Mitchell (1988a), Dissociative recombination of electrons with H_2^+ in low vibrational states, *Phys. Rev. Lett.*, *60*, 1006–1009.

Hus, H., F. Youssif, A. Sen, and J. B. A. Mitchell (1988b), Merged-beam studies of the dissociative recombination of H_3^+ ions with low internal energy, *Phys. Rev. A*, *38*(2), 658–663.

Johnsen, R. (1987), Microwave afterglow measurements of the dissociative recombination of molecular ions with electrons, *Int. J. Mass Spectrosc. Ion Processes*, *81*, 67.

Kasner, W. H. (1967), Study of the temperature dependence of electron-ion recombination in nitrogen, *Phys. Rev.*, *164*, 194–200.

Kella, D., P. J. Johnson, H. B. Pedersen, L. Vejby-Christensen, and L. H. Andersen (1996), Branching ratios for dissociative recombination of $^{15}N^{14}N^+$, *Phys. Rev. Lett.*, *77*, 2432–2435.

Kella, D., L. Vejby-Christensen, P. J. Johnson, H. B. Pedersen, and L. H. Andersen (1997), The source of green light emission determined from a heavy-ion storage ring experiment, *Science*, *276*, 1530–1533.

Keyser, C. J., H. R. Froelich, J. B. A. Mitchell, and J. W. McGowan (1979), Beam-scanning system for determination of beam profiles and form factors in merged-beam experiments, *J. Phys. E Sci. Instrum.*, *12*, 316–320.

Killeen, T. L., and P. B. Hays (1983), O(^{1}S) from dissociative recombination of O_2^+: Nonthermal line profile measurements from Dynamics Explorer, *J. Geophys. Res.*, *88*, 10,163–10,169.

Kley, D., G. M. Lawrence, and E. J. Stone (1977), The yield of N(2D) atoms in dissociative recombination of NO^+, *J. Chem. Phys.*, *66*, 4157.

Larson, A., et al. (1998), Branching fractions in dissociative recombination of CH_2^+, *Astrophys. J.*, *505*, 459–465.

Larson, A., et al. (2000), Resonant ion-pair formation in electron collisions with HD^+ and OH^+, *Phys. Rev.*, *62*, 042707-1–042707-8.

Lee, C. M. (1977), Multichannel dissociative recombination theory, *Phys. Rev. A*, *16*, 109–122.

Le Padellec, A. N., C. Sheehan, D. Talbi, and J. B. A. Mitchell (1997), A merged-beam study of the dissociative recombination of HCO^+, *J. Phys. B At. Mol. Opt. Phys.*, *30*, 319–327.

Le Padellec, A., C. Sheehan, and J. B. A. Mitchell (1998), The dissociative recombination of CN+, $^+$, *J. Phys. B At. Mol. Opt. Phys.*, *31*, 1725–1728.

Le Padellec, A., J. B. A. Mitchell, A. Al-Khalili, H. Danared, A. Kallberg, A. Larson, S. Rosen, M. af Ugglas, L. Vikor, and M. Larsson (1999), Storage ring measurements of the dissociative recombination and excitation of the cyanogens ion CN^+ ($X^1\Sigma^+$ and $a^3\Pi$, v = 0), *J. Chem. Phys.*, *110*, 890–901.

Le Padellec, A., et al. (2001), Resonant ion-pair formation in the recombination of NO+ with electrons: Cross-section determination, *Phys. Rev. A*, *64,* 012702-7012702-7.

Lilensten, J., and P.-L. Blelly (1999), *Du Soleil à la Terre: Aéronomie et Météorologie de L'Espace*, Presses Univ. de Grenoble, Grenoble, France.

Linderberg, J. (1998), Dissociative recombination: An electronic correlation problem, *Mol. Phys.*, *94*, 99–104.

Lindinger, W., F. Howorka, P. Lukac, S. Kuhn, H. Villinger, E. Alg, and H. Ramler (1981), Charge transfer of $Ar^+ + N_2 \rightarrow N_2^+ + Ar$ at near thermal energies, *Phys. Rev. A*, *23*, 2319–2326.

Mahdavi, M. R., J. B. Hasted, and M. M. Nakshbandi (1971), Electron-ion recombination measurements in the flowing afterglow, *J. Phys. B At. Mol. Opt. Phys.*, *4*, 1726–1737.

McDaniel, E. W., J. B. A. Mitchell, and M. E. Rudd (1993), *Atomic Collisions: Heavy Particle Projectiles*, John Wiley, Hoboken, N. J.

McNeil, W. J., R. A. Dressler, and E. Murad (2001), Impact of a major meteor storm on Earth's ionosphere: A modeling study, *J. Geophys. Res.*, *106*, 10,447–10,466.

Mehr, F. J., and M. A. Biondi (1969), Electron temperature dependence of recombination of O_2^+ and N_2^+ ions with electrons, *Phys. Rev.*, *181*, 264–271.

Michels, H. H. (1975), Air Force Cambridge Research Laboratory Report, *AFCRL-TR-75-050*, Air Force Cambridge Res. Lab., Hanscom Air Force Base, Mass.

Mitchell, J. B. A. (1990), The dissociative recombination of molecular ions, *Phys. Rep.*, *186*, 215–248.

Mitchell, J. B. A. (2001), Dissociative recombination and excitation in fusion edge plasmas, *At. Plasma Mater. Interact. Data*, *9*.

Mitchell, J. B. A., and C. Rebrion-Rowe (1997), The recombination of electrons with complex molecular ions, *Int. Rev. Phys. Chem.*, *16*, 201–213.

Mostefaoui, T., S. Laube, G. Gautier, C. Rebrion-Rowe, B. R. Rowe, and J. B. A. Mitchell (1999), The dissociative recombination of NO^+: The influence of the vibrational excitation state, *J. Phys. B At. Mol. Opt. Phys.*, *32*, 5247–5256.

Mul, P. M., and J. W. McGowan (1979), Merged electron-ion beam experiments. III. Temperature dependence of dissociative recombination for atmospheric ions NO^+, O_2^+ and N_2^+, *J. Phys. B At. Mol. Opt. Phys.*, *12*, 1591–1602.

Noren, C., F. B. Yousif, and J. B. A. Mitchell (1989), Dissociative recombination and excitation of N_2^+, *J. Chem. Soc. Faraday Trans. 2*, *85*, 1697–1703.

Oddone, S., J. W. Sheldon, and K. A. Hardy (1997), Dissociative recombination of the $A^2\Pi_u$ and the $X^2\Sigma_g$ states of N_2^+ in a glow discharge, *Phys. Rev. A*, *56*, 4737–4741.

Peek, J. M., A. R.-Hashemi-Attar, and C. L. Beckel (1979), Spontaneous emission lifetimes in the ground electronic states of HD^+ and H_2^+, *J. Chem. Phys.*, *71*, 5382–5383.

Peterson, J. R., et al. (1998), Dissociative recombination and excitation of N_2^+: Cross sections and product branching ratios, $^+$, *J. Chem. Phys.*, *108*, 1978–1988.

Peverall, R., et al. (2000), The ionospheric oxygen green airglow: Electron temperature dependence and aeronomical implications, *Geophys. Res. Lett.*, *27*, 481–484.

Peverall, R., et al. (2001), Dissociative recombination and excitation of O_2^+: Cross sections, product yields and implications for studies of ionospheric airglows, *J. Chem. Phys.*, *114*, 6679–6689.

Phaneuf, R. A., C. C. Havener, G. H. Dunn, and A. Muller (1999), Merged-beams experiments in atomic and molecular physics, *Rep. Prog. Phys.*, *62*, 1143–1180.

Queffelec, J. L., B. R. Rowe, F. Vallee, J. C. Gomet, and M. Morlais (1989), The yield of metastable atoms through dissociative recombination of O_2^+ ions with electrons, *J. Chem. Phys.*, *91*, 5335–5342.

Rabadan, I., and J. Tennyson (1996), R-matrix calculation of the bound and continuum states of the e^--NO^+ system, *J. Phys. B At. Mol. Opt. Phys.*, *29*, 3747–3761.

Rabadan, I., and J. Tennyson (1997), Ab initio potential energy curves of Rydberg, valence and continuum states of NO^+, *J. Phys. B At. Mol. Opt. Phys.*, *30*, 1975–1988.

Rabadan, I., and J. Tennyson (1998), Ab initio potential energy curves of Rydberg, valence and continuum states of NO^+ (corrigendum), *J. Phys. B At. Mol. Opt. Phys.*, *31*, 4485–4487.

Rees, M. H. (1989), *Physics and Chemistry of the Upper Atmosphere*, Cambridge Univ. Press, New York.

Schlegel, K. (1982), Reduced effective recombination coefficient in the disturbed polar E region, *J. Atmos. Terr. Phys.*, *44*, 183–185.

Schlegel, K., and J. P. St.-Maurice (1981), Anomalous heating of the polar E region by unstable plasma waves: 1. Observations, *J. Geophys. Res.*, *86*, 1447–1452.

Schmidt, H. T., L. Vejby-Christensen, H. B. Pedersen, D. Kella, N. Bjerre, and L. H. Andersen (1996), Dissociated recombination of vibrationally excited H_2^+ ions: The effect of laser photodissociation on the initial vibrational distribution, *J. Phys. B At. Mol. Opt. Phys.*, *29*, 2485–2496.

Schneider, I. F., C. Stromholm, L. Carata, X. Urbain, M. Larsson, and A. Suzor-Weiner (1997), Rotational effects in HD^+ dissociative recombination: Theoretical study of resonant mechanisms and comparison with ion storage ring experiments, *J. Phys. B At. Mol. Opt. Phys.*, *30*, 2687–2705.

Schneider, I. F., I. Rabadan, L. Carata, L. H. Andersen, A. Suzor-Weiner, and J. Tennyson (2000), Dissociative recombination of NO^+: Calculations and comparison with experiment, *J. Phys. B At. Mol. Opt. Phys.*, *33*, 4849–4861.

Schunk, R. W., and A. F. Nagy (1980), Ionospheres of the terrestrial planets, *Rev. Geophys.*, *18*, 813–851.

Schunk, R. W., and A. F. Nagy (2000), *Ionospheres: Physics, Plasma Physics, and Chemistry*, Cambridge Univ. Press, New York.

Sheehan, C. H. (1996), A merged beam analysis of the dissociative recombination of helium hydride ions, M.Sc. thesis, Univ. of Western Ontario, London, Ontario, Canada.

Sheehan, C. H. (2000), A merged beam analysis of the dissociative recombination of molecular ions of importance to ionospheric and interstellar chemistry, Ph.D. thesis, Univ. of Western Ontario, London, Ontario, Canada.

Sheehan, C. H., and J.-P. St.-Maurice (2004), The dissociative recombination of the methane family ions: Rate coefficients and implications, *Adv. Space Res.*, in press.

Sheehan, C., A. Le Padellec, W. N. Lennard, D. Talbi, and J. B. A. Mitchell (1999), Merged beam measurement of the dissociative recombination of HCN^+ and HNC^+, *J. Phys. B At. Mol. Opt. Phys.*, *32*, 3347–3360.

Sheehan, C., W. J. Lennard, and J. B. A. Mitchell (2000), Measurement of the efficiency of a silicon surface barrier detector for medium energy ions using a Rutherford backscattering experiment, *Meas. Sci. Technol.*, *11*, L5–L7.

Smith, D., and N. G. Adams (1981), Charge-transfer reaction $Ar^+ + N_2 \rightarrow N_2^+ + Ar$ at thermal energies, *Phys. Rev. A*, *23*, 2327–2330.

Sobral, J. H. A., H. Takahashi, M. A. Abdu, P. Muralikrishna, Y. Sahai, and C. J. Zamlutti (1992), $O(^1S)$ and $O(^1D)$ quantum yields from rocket measurements of electron densities and 557.7 and 630.0 nm emissions in the nocturnal F-region, *Planet. Space Sci.*, *40*, 607–609.

Spanel, P., L. Dittrichova, and D. Smith (1993), FALP studies of the dissociative recombination coefficients for O_2^+ and NO^+ with electrons in the temperature range 300 K to 2000 K, *Int. J. Mass Spectrom. Ion Processes*, *129*, 183–191.

St.-Maurice, J.-P., K. Schlegel, and P. M. Banks (1981), Anomalous heating of the polar E region by unstable plasma waves: 2. Theory, *J. Geophys. Res.*, *86*, 1453–1462.

St.-Maurice, J.-P., C. Cussenot, and W. Kofman (1999), On the usefulness of E region electron temperatures and lower F region ion temperatures for the extraction of thermospheric parameters: A case study, *Ann. Geophys.*, *17*, 1182–1198.

Sun, H., and H. Nakamura (1990), Theoretical study of the dissociative recombination of NO^+ with slow electrons, *J. Chem. Phys.*, *93*, 6491–6501.

Takahashi, H., B. R. Clemensa, P. P. Batista, Y. Sahai, M. A. Abdu, and P. Muralikrishna (1990), Equatorial F-region O1 6300 A and O1 5577 A emission profiles observed by rocket-borne airglow photometers, *Planet. Space Sci.*, *38*, 547–554.

Talbi, D., A. Le Padellec, and J. B. A. Mitchell (2000), Quantum chemical calculations for the dissociative recombination of HCN^+ and HNC^+, *J. Phys. B At. Mol. Opt. Phys.*, *33*, 3631–3646.

Valcu, B., I. F. Schneider, M. Raoult, C. Stromholm, M. Larsson, and A. Suzor-Weiner (1998), Rotational effects in low energy dissociative recombination of diatomic ions, *Eur. Phys. J. D*, *1*, 71–78.

Van der Donk, P., F. B. Yousif, J. B. A. Mitchell, and A. P. Hickman (1991), Dissociative recombination of H_2^+, *Phys. Rev. Lett.*, *67*, 25–42.

Vejby-Christensen, L., L. H. Andersen, O. Heber, D. Kella, H. B. Pedersen, H. T. Schmidt, and D. Zajfman (1997), Complete branching ratios for the dissociative recombination of H_2O^+, H_3O^+, and CH_3^+, *Astrophys. J.*, *483*, 531–540.

Vejby-Christensen, L., D. Kella, H. B. Pedersen, and L. H. Andersen (1998), Dissociative recombination of NO^+, *Phys. Rev. A*, *57*, 3627–3634.

Walls, F. L., and G. H. Dunn (1974), Measurements of total cross sections for electron recombination with NO^+ and O_2^+ using ion storage techniques, *J. Geophys. Res.*, *79*, 1911.

Weller, C. S., and M. A. Biondi (1968), Recombination, attachment, and ambipolar diffusion of electrons in photo-ionized NO afterglows, *Phys. Rev.*, *172*, 198–206.

Wickwar, V. B., C. Lathuillere, W. Kofman, and G. Lejeune (1981), Elevated electron temperatures in the auroral E layer measured with the Chatanika radar, *J. Geophys. Res.*, *86*, 4721–4730.

Yee, J.-H., V. J. Abreu, and W. B. Colwell (1989), Aeronomical determination of the quantum yields of $O(^1S)$ and $O(^1D)$ from dissociative recombination of O_2^+, in *Dissociative Recombination: Theory, Experiment, and Applications*, edited by J. B. A. Mitchell and S. L. Guberman, p. 286, World Sci., River Edge, N. J.

Young, R. A., and G. St. John (1966), Recombination coefficient of NO^+ with e, *Phys. Rev.*, *152*, 25–28.

Zajfman, D., and Z. Amitay (1995), Measurement of the vibrational populations of molecular ions and its application to dissociative recombination in storage rings, *Phys. Rev. A*, *55*, 839–842.

Zhang, S.-R., W. L. Oliver, S. Fukao, and Y. Otsuka (2000), A study of the forenoon ionospheric F_2 layer behavior over the middle and upper atmospheric radar, *J. Geophys. Res.*, *105*, 15,823–15,833.

Zipf, E. C. (1980a), The dissociative recombination of vibrationally excited N_2^+ ions, *Geophys. Res. Lett.*, *7*, 645–648.

Zipf, E. C. (1980b), A laboratory study on the dissociative recombination of vibrationally excited O_2^+ ions, *J. Geophys. Res.*, *85*, 4232–4236.

Zipf, E. C. (1988), The excitation of the $O(^1S)$ state by the dissociative recombination of O_2^+ ions: electron temperature dependence, *Planet. Space Sci.*, *36*, 621–628.

Zong, W., et al. (1999), Resonant ion pair formation in electron collisions with ground state molecular ions, *Phys. Rev. Lett.*, *83*, 951–954.

C. H. Sheehan, Department of Physics, Ouachita Baptist University, 410 Ouachita Street, Arkadelphia, AR 71998-0001, USA. (sheehanc@obu.edu)

J.-P. St.-Maurice, Department of Physics and Astronomy, University of Western Ontario, London, Ontario N6A 3K7, Canada. (jstmauri@uwo.ca)